



# Reliability of pedotransfer functions and field-saturated hydraulic conductivity prediction for agricultural soils in Zambia, Africa

---

Yannic Janal

Master's Degree

Swedish University of Agricultural Sciences, SLU

Faculty of Natural Resources and Agricultural Sciences, Department of Soil and Environment

Environmental Science - Soil, Water and Biodiversity (EnvEuro) Programme

Examensarbeten/Institutionen för mark och miljö, SLU

Part number: 2024:20

Uppsala 2024



# Reliability of pedotransfer functions and field-saturated hydraulic conductivity prediction for agricultural soils in Zambia, Africa

Yannic Janal

**Supervisor:** Jennie Barron, Swedish University of Agricultural Sciences, Department of Soil and Environment  
**Assistant supervisor:** Christine Stumpp, BOKU University, Department of Water, Atmosphere and Environment (WAU)  
**Examiner:** Erik Karlton, Swedish University of Agricultural Science, Department of Soil and Environment

**Credits:** 30 credits  
**Level:** A2E  
**Course title:** Master thesis in Environmental science, A2E  
**Course code:** EX0897  
**Programme/education:** Environmental Science - Soil, Water and Biodiversity (EnvEuro)  
**Course coordinating dept:** Department of Aquatic Science and Assessment  
**Place of publication:** Uppsala, Sweden  
**Year of publication:** 2024  
**Copyright:** This work is licensed under CC BY-NC 4.0 (<https://creativecommons.org/licenses/by-nc/4.0/>)  
The illustrations are created by the author, unless otherwise indicated. Cover illustration: Author discusses with colleague during field sampling, 2024.

**Keywords:** Sub-Saharan Africa, water retention, in-situ field measurements, smallholder farming, conventional farming, Land Degredation Surveillance Framework

**Swedish University of Agricultural Sciences**  
Faculty of Natural Resources and Agricultural Sciences  
Department of Soil and Environment

## Abstract

Farming in Sub-Saharan Africa is expected to be faced with more frequent droughts and storms. Most farming systems lack the infrastructure to cope with such extreme events, and rely on soil water retention and soil hydraulic conductivity to store water while allowing stormwater to infiltrate. However, research on improving soil hydraulic properties in this region has been limited due to scarce funding and resources. Pedotransfer functions (PTFs), which use easily measurable and more often readily available parameters to predict hydraulic characteristics, offer potential solutions, but only limited numbers of PTF have been developed or tested for Sub-Saharan Africa specifically. This study aims to evaluate soil hydraulic properties of agricultural soils using PTFs in Zambia (southern Africa). Twelve existing PTFs were tested on their accuracy to predict field-saturated hydraulic conductivity ( $K_{fs}$ ) and water retention. Therefore, 32 fields in 3 districts and 2 farming systems (small-scale and commercial farms) were sampled for soil texture, organic matter, bulk density, water retention and  $K_{fs}$  in top and subsoil.

The results revealed higher and more spatially varying infiltration rates on commercial farms (about twice the rate), while showing significantly higher clay content (mean= 40%). A reason might be the formation of cracks and different soil management practices like tillage, impacting soil structure and determining  $K_{fs}$ . Further robust driving factors were difficult to determine. PTFs predicting  $K_{fs}$  were scarce and the ones existing failed to adequately predict  $K_{fs}$ . Obtained agreements of PTF estimated and field measured field capacity (-10kPa) ranged between  $-0.21 < R < 0.41$  (top-soil) and  $-0.71 < R < 0.40$  (sub-soil), while permanent wilting point (-1500kPa) varied within ranges of  $-0.45 < R < 0.49$  (top-soil) and  $-0.69 < R < 0.42$  (sub-soil). Notably, permanent wilting points at  $>0.15$  vol% were performing poorly possibly due to lab analysis errors at high pressures. My results highlight the need to go beyond basic soil parameters for determining hydraulic soil properties, and a need to further build soil data from field sampling to improve PTFs applicability for agricultural soils in Zambia.

*Keywords:* Sub-Saharan Africa, water retention, in-situ field measurements, smallholder farming, conventional farming, Land Degradation Surveillance Framework

# Table of contents

<b>List of tables .....</b>	<b>5</b>
<b>List of figures.....</b>	<b>6</b>
<b>Abbreviations .....</b>	<b>8</b>
<b>1. Introduction .....</b>	<b>9</b>
<b>2. Material &amp; Methods .....</b>	<b>12</b>
2.1 Sampling design & data collection .....	12
2.2 Determination of hydraulic properties .....	16
2.3 Pedotransfer function selection.....	18
2.4 Statistical validation .....	20
2.5 Missing data .....	21
<b>3. Results .....</b>	<b>23</b>
3.1 Site description.....	23
3.2 Predictors for field-saturated hydraulic conductivity .....	28
3.3 Accuracy of selected pedotransfer functions .....	28
3.4 Sensitivity of selected pedotransfer functions.....	31
<b>4. Discussion .....</b>	<b>35</b>
<b>References .....</b>	<b>37</b>
<b>Popular science summary.....</b>	<b>42</b>
<b>Acknowledgements.....</b>	<b>43</b>

# List of tables

Table 1: Selected pedotransfer functions to be tested with the Zambian agricultural soils. $\theta_{\psi}$ : water retention curve (as soil water content $\theta_m$ at a certain negative pressure $m$ (unit: kPa)), $\theta_{-10, -1500}$ water content at negative pressure levels -10 and -1500, $K_{fs}$ : field-saturated hydraulic conductivity, cl: clay, si: silt, sa: sand, OC: organic carbon, BD: bulk density, CEC: cation exchange capacity and EP: effective porosity.....	19
Table 2: Range of the pedotransfer function training data-set for texture variables. x: no data given in the literature, -: variable not in the function.....	19
Table 3: Chemical and physical data of the sampling sites per A horizon as well as the p-values to determine significant differences between districts (Kalomo, Lusaka and Katete). n: number of samples, OC: organic carbon, BD: bulk density, CEC: cation exchange capacity, N: nitrogen, $\theta$ : water content at pressure level -10 kPa or -1500 kPa, x: insufficient data of all districts.....	25
Table 4: Chemical and physical data of the sampling sites per B horizon as well as the p-values to determine significant differences between districts (Kalomo, Lusaka and Katete). n: number of samples, OC: organic carbon, BD: bulk density, CEC: cation exchange capacity, N: nitrogen, $\theta$ : water content at pressure level -10 kPa or -1500 kPa, x: insufficient data of all districts.....	25
Table 5: Evaluation of the predicted field-saturated hydraulic conductivity ( $K_{fs}$ ) for top-soil (horizon A). .....	29
Table 6: Evaluation of the predicted water retention at field capacity (-10 kPa) and permanent wilting point (-1500 kPa) per horizon A and B.....	30

# List of figures

Figure 1: Graphic overview of the material and applied methods. RQ1 represents the regression analysis of research question 1 and RQ2 the regression analysis, model validation and sensitivity analysis of research question 2. $K_{fs}$ : field-saturated hydraulic conductivity, ME: mean error, RMSE: root mean square error. ....	12
Figure 2: Map of the 3 study areas Kalomo, Lusaka and Katete and the sample locations in the area. Adopted from Emmanuel Ngonga. ....	14
Figure 3: Images of some sampling process in the field. Left: loose soil sampling with an auger for chemical analysis, centre: soil cylinders halfway inserted for bulk density, right: infiltration rate measurement with an inserted infiltration tube, a fixed rule. ....	14
Figure 4: Example of field-saturated hydraulic conductivity ( $K_{fs}$ ) determination. $K_{fs}^i$ represents an intermediate value where saturation has not fully occurred. $K_{fs}$ represents the final value used for further assessments. $K_{fs}$ : field-saturated hydraulic conductivity. ....	17
Figure 5: Boundaries of the selected PTF texture input parameters in a texture triangle. If no boundary was given, a boundary of 100% was assumed for the respective value. "Adhikary_pF": Adhikary et al. ( $\theta$ ). ....	20
Figure 6: 3 scenarios for the sensitivity analysis, showing the extent of variations on a texture triangle. In scenario "texture 1" and "texture 2" only the texture content is varied while all other variables are kept constant. In scenario "OC" only the organic carbon (OC) content is varied. ....	22
Figure 7: Graphical disaggregation of selected soil properties per district (Kalomo, Lusaka and Katete) and horizon (A and B). OC: organic carbon, BD: bulk density. ....	24
Figure 8: Graphical disaggregation of hydraulic properties per district (Kalomo, Lusaka and Katete) and horizon (A and B). -10 kPa: field capacity, -1500 kPa: permanent wilting point. ....	26
Figure 9: Field-saturated hydraulic conductivity ( $K_{fs}$ ) results per location (Katete, Kalomo and Lusaka). Top: Mean infiltration rates with 95% confidence interval of the 3-4 repeated infiltration measurements. Centre: statistical results from the curve	

fitting procedure to estimate the randomness of measured points. Bottom: final $K_{fs}$ distribution per field and per district.....	27
Figure 10: Simple linear regression plots of selected variables and field-saturated hydraulic conductivity ( $K_{fs}$ ) at horizon A. The regression line shown in the plots was calculated across all districts but only for horizon A. OC: organic carbon, BD: bulk density.....	28
Figure 11: Performance of pedotransfer functions which return field-saturated hydraulic conductivity ( $K_{fs}$ ) for top-soil (horizon A) conditions. The grey line represents the line of perfect agreement where points would lie if the predictions exactly matched the observations.....	29
Figure 12: Performance of pedotransfer functions which return the water content ( $\theta$ ) for top-soil (horizon A) conditions. The grey line represents the line of perfect agreement where points would lie if the predictions exactly matched the observations.....	30
Figure 13: Sensitivity analysis of pedotransfer functions which return field-saturated hydraulic conductivity values. The y-axis represents the variation in field-saturated hydraulic conductivity.....	32
Figure 14: Sensitivity analysis of pedotransfer functions which return water retention values. The y-axis represents the variation in water content given by the functions. OC: organic carbon.....	34

## Abbreviations

BD	Bulk density
CEC	Cation exchange capacity
cl	Clay
FC	Field capacity
$K_{fs}$	Field-saturated hydraulic conductivity
LDSF	Land Degradation Surveillance Framework
ME	Mean error
N	Nitrogen
OAT	One-at-a-time sensitivity analysis
OC	Organic carbon
P	Porosity
pF	Water retention curve
PTF	Pedotransfer function
PWP	Permanent wilting point
R	Pearson correlation coefficient
RMSE	Root mean square error
RQ1	Research question 1
RQ2	Research question 2
sa	Sand
si	Silt
UNZA	University of Zambia
USDA	United States Department of Agriculture
ZARI	Zambian Agricultural Research Institute
$\theta$	Water content
$\psi$	Matric potential



# 1. Introduction

Water scarcity is a pressing issue in Sub-Saharan Africa, putting the well-being of roughly 90 million Africans at immediate risk in 2022 (EM-DAT & CRED 2024). Driven by a combination of factors including rainfall deficits, population growth and poor infrastructure, governments have struggled to find adequate solutions despite being on the international agenda for decades (Nkiaka et al. 2021). The increase of global temperatures adds to the fragile situation. Temperature shocks, changes in precipitation patterns and more intense weather events causes irregular water availability and increased stress on crops and soils (IPCC 2022). Sub-Saharan Africa is projected to be the region most affected by climate change impacts globally, with the largest number of water-stressed countries (Adepoju 2021).

In Zambia, a country located in Sub-Sahara Africa, agricultural productivity directly determines economic performance and social stability. Twenty-two percent of Zambians were working in the agricultural sector in 2022 and around 85% of Zambians depended on farming for their livelihoods (Zambia Statistics Agency 2023; Chikowo 2024; World Bank 2024a). The vast majority are smallholder farmers who conduct rain-fed agriculture and, as such, are particularly vulnerable to droughts (Silva et al. 2023). Smallholder farmers in Zambia typically employ traditional farming practices: labour intensive, small-scale and the usage of harvest for food, feed, energy and as building material. Limited financial capacities, poor knowledge and insecure land tenure often do not allow for adequate fertilization, application of pesticides and herbicides and the installation of irrigation infrastructure (Ngoma et al. 2019).

Numerous studies have highlighted the role of soils and soil health in storing rainwater and in providing plant-available water over dry periods (Rockström et al. 2010; Jägermeyr et al. 2016; Lehmann et al. 2020). Sandy soils for example drain quickly and hold little water while clay soils retain water beyond the plants retrieving capacities. Loamy soils provide a balance between good water retention and drainage for plant roots but adjusting soil texture is very costly in practice. Furthermore, by increasing the content of soil organic carbon, water content at various soil moisture levels improves, particularly in sandy soils, though the overall effect on available water capacity is modest (Minasny & McBratney 2018). However, implementing soil organic carbon promoting practices requires the input of biomass to the soil, which may compete against other usages of biomass in

smallholder farming. Other important properties are soil bulk density and aggregate stability, both significantly affected by tillage and crop management. Moderate density and stable aggregates form structures allowing water to infiltrate and be stored in the pores while maintaining resistance to soil erosion (Basset et al. 2023). Farming practices with heavy machinery and regular tillage are prone to compact soils and degrade aggregates. Therefore, applying the right farming practice for the right environment and soil is a difficult task especially given the limited knowledge on smallholder farming in Sub-Saharan Africa (Bargués-Tobella et al. 2024).

Soil moisture dynamics in agricultural soils are governed by hydraulic parameters such as hydraulic conductivity and soil water retention. Soil field-saturated hydraulic conductivity ( $K_{fs}$ ) describes the rate with which water can move through soil pores at saturation measured in the field (contrary to the more disturbed measurements in the laboratory) and is governed by factors such as soil texture, soil structure and organic matter content. It is a key variable for determining rainwater infiltration, runoff and sub-surface water recharge (Vereecken et al. 2010). Soil water retention measures the soil's ability to retain water against the force of gravity, affecting plant-available water (soil moisture) in the rootzone. However, both parameters are notorious for being time consuming to measure, expensive and often depend on the scale of the sampling and of the analysis. Open data on soil related hydraulic properties for Zambia are scarce, especially data directly measured in the fields. This is further complicated by the lack of standardized sampling methods, decreasing the liability of old data (Mukumbuta et al. 2021). Therefore, many studies apply prediction tools to estimate  $K_{fs}$  and soil water retention (Van Looy et al. 2017). Pedotransfer functions (PTFs) are commonly used for that purpose. They link easily measurable and more often readily available soil properties like texture, bulk density and carbon content to hydraulic characteristics. The drawback of PTFs comes in the application for different soil classes and climatic zones: since they are trained on soil parameter of certain areas, their estimation accuracy significantly decreases when applied elsewhere. Globally, more soil research has been conducted in temperate regions (Hartemink 2002). Sub-Saharan Africa has seen little PTF development (Young et al. 1999; Miti et al. 2023). Several attempts have been made in the past but lacked the sampling numbers for broad application (Pidgeon 1972; Lal 1978; Karlsson 1982; Aina & Periaswamy 1985). Recent PTFs compensate the sampling issues by including open data, however, given the size and variability of the continent, are still limited to sections of countries and few selected areas of interest (Kalumba et al. 2021; Myeni et al. 2021; Teferi et al. 2023). Another option would be to apply PTFs from other continents with the same agro-ecological zones or soils. Miti et al. (2023) has found correlations between selected tropical PTFs and legacy data (legacy data refers to peer-reviewed publications, MSc and PhD theses, internal reports and the World Soil Information Service database) in

Zambia. Yet, it remains open to what extent existing PTFs are applicable for agricultural soils in Zambia and if they can differentiate between types of farming.

This study aims to determine whether PTFs can be used to develop soil hydraulic properties for agricultural (crop) land in Zambia using easily available soil properties such as texture, bulk density and organic carbon. To do this, I sampled 32 farms at 3 clusters and 2 soil depths, measured in-situ  $K_{fs}$  following the Land Degradation Surveillance Framework, a standardized sampling method used across Africa, measured field capacity and permanent wilting point for water retention properties, and measured texture, bulk density, and organic matter. Furthermore, I identified a number of PTFs potentially relevant for Zambia's soil conditions and explored the sensitivity in the PTF input variables for the soil sample range.

Two lead research questions were determined:

1. What are driving factors for soil field-saturated hydraulic conductivity ( $K_{fs}$ ) on agricultural soils in Zambia? (RQ1)
2. Which existing pedotransfer functions (PTF) for  $K_{fs}$  and water retention are suitable for agricultural soils in Zambia and how sensitive are they to changes? (RQ2)

## 2. Material & Methods

A graphic overview of the methodical workflow is depicted in Figure 1. In the following, details on the material and applied methods are provided.

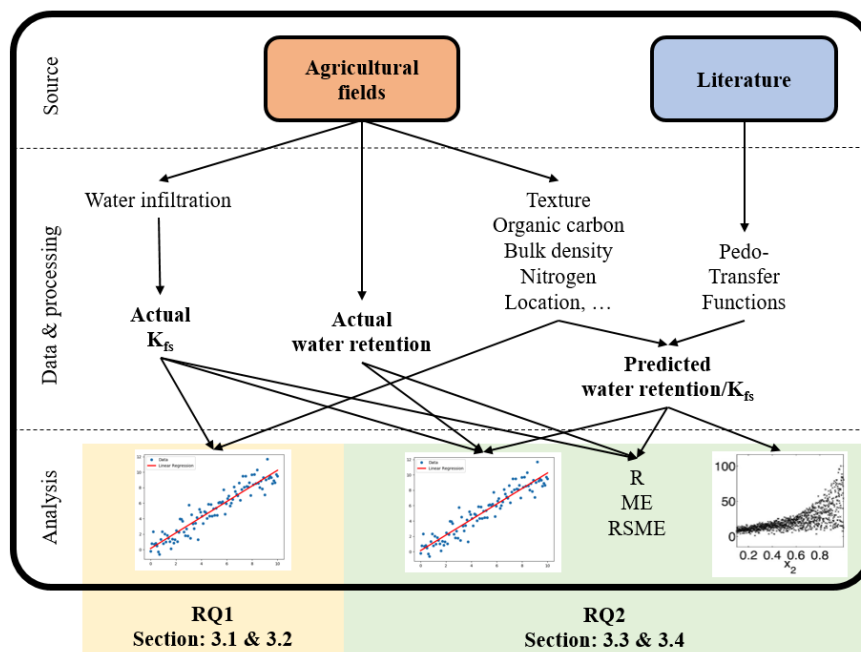


Figure 1: Graphic overview of the material and applied methods. RQ1 represents the regression analysis of research question 1 and RQ2 the regression analysis, model validation and sensitivity analysis of research question 2.  $K_{fs}$ : field-saturated hydraulic conductivity, ME: mean error, RMSE: root mean square error.

### 2.1 Sampling design & data collection

The methods applied in the field are determined by the sampling design. In this study, the sampling design follows the Land Degradation Surveillance Framework (LDSF), a standardized approach to ensure representative and comparable results across the world (Tamene et al. 2019; Vågen & Winowiecki 2023; Bargués-Tobella et al. 2024). While it was initially created for assessing soil and land health, its

inexpensive and simple to use methods can be applied individually for many situations. According to the LDSF sampling procedure, the site is divided into 16 2.5km by 2.5km tiles. Within each tile, an area of 1km<sup>2</sup> is selected and 10 random sampling plots generated, each divided into 4 circular sub-plots of 100m<sup>2</sup> size. The sub-plots are positioned in a triangular way, hence 1 sub-plot forms the centre and 3 surround the centre sub-plot by a 120 degree angle. For this study, this procedure had to be abbreviated due to time and resource constraints: instead of 16 tiles and areas, only 1 area in each district (of 25km<sup>2</sup> in Kalomo and 150km<sup>2</sup> in Lusaka and Katete) was selected. Furthermore, each sampling plot was not randomly placed but pre-selected in such a way, that most of the area was covered. It should be noted however, that the location of the areas and plots was largely influenced by the availability of agricultural fields, willingness of the farmers to participate and accessibility. In total, I positioned 32 plots: 10 in Kalomo, 12 in Lusaka (2 additional plots had to be added due to varieties in the fields) and 10 in Katete (see Figure 2). These regions were chosen because they collectively accounted for over half of the agricultural yields in 2019 (Teschemacher et al. 2024). Sampling took place between February and April 2024.

General information on the field was partly gathered from the farmers and partly measured. Information provided by farmers included: crop variety and management related information such as crop rotation application, irrigation regime, fertilization regime, weeding and pest management. Information measured in the field included: field coordinates. Horizons were determined in the field by analysing soil color and by determining texture using the feel method. By that, the highly management-affected top-soil was differentiated from sub-soil.

Chemical data was collected following the LDSF guide on composite soil sampling. At the centre of each sub-plot a sample was taken using an auger (see Figure 3). All sub-plot samples were then mixed, creating one composite sample per plot. This process was repeated for each horizon, hence at the depth 0-10cm and 30-40cm for soils with 2 horizons (28 fields showed 2 horizons) and 0-10cm, 20-30cm and 40-50cm for soils with 3 horizons (4 fields in Lusaka showed 3 horizons). Notably, in 2 instances an error was made and instead of sampling 0-10cm it was sampled 0-30cm. The composite samples were then taken to the Zambian Agriculture Research Institute (ZARI), a government funded laboratory, for further processing. Each sample was air-dried and sieved through a 2 mm mesh to remove debris and larger particles. The prepared samples were then stored in labelled, airtight containers until further analysis. Organic carbon was determined using the Walkley-Black method (GLOSOLAN 2019), a procedure where organic carbon is oxidized and calculated from the amount of chromate ions formed using a colorimetric procedure. Texture was measured using a hydrometer, which uses the difference in specific gravity of the particle size. It involves dispersing a soil sample in a sodium hexametaphosphate solution to break apart aggregates, shaking the

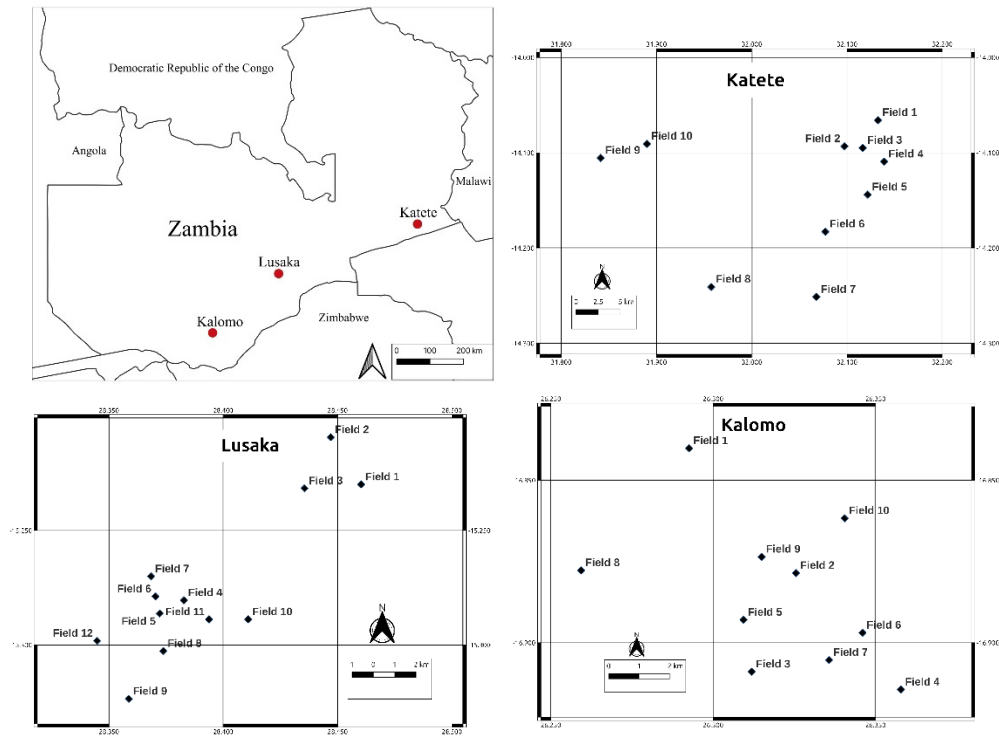


Figure 2: Map of the 3 study areas Kalomo, Lusaka and Katete and the sample locations in the area. Adopted from Emmanuel Ngonga.



Figure 3: Images of some sampling process in the field. Left: loose soil sampling with an auger for chemical analysis, centre: soil cylinders halfway inserted for bulk density, right: infiltration rate measurement with an inserted infiltration tube, a fixed rule.

solution in a sediment cylinder filled with distilled water to ensure uniform distribution and to measure the concentration of suspended material which correspond to the settling velocities of sand, silt and clay particles. The available equipment at ZARI allowed increments of 5% texture content, thus measurements were recorded as 0%, 5%, 10% and so on up to 100%. For the texture classes the United States Department of Agriculture (USDA) classification was applied, which defines the size of sand (2-0.05mm), silt (0.05-0.002mm) and clay (<0.002mm). pH was determined using CaCl, cation exchange capacity (CEC) was measured with the ammonium acetate method of Schollenberg and Drelbelbis (Schollenberger & Simon 1945) and nitrogen (N) was determined using the Kjeldahl method (Kjeldahl 1883).

Bulk density data was determined using the core sample method (see Figure 3). Thereby, a steel cylinder of pre-defined volume ( $98.17\text{cm}^3$ ) was placed on the soil, covered with a wooden plank, inserted in the soil by gently hammering on the wooden plank with a mallet until the cylinder top reached the soil surface, the sides dug out, sealed on the bottom with a trowel by pushing the trowel in the soil from the side, pulled out, cleaned and put into a labelled plastic bag. This procedure was repeated 4 times per horizon and field and was always located on the centre sub-plot. The following depths were sampled: 0-5cm and 30-35cm for soils with 2 horizons (horizon A and B) and 0-5cm, 20-25cm, 40-45cm for soils with 3 horizons (horizon A, B<sub>int</sub>, B). Afterwards the samples were taken to ZARI for drying in the oven and for determining the mass. By dividing the mass with the cylinder volume, the soil bulk density per sub-plot was expressed. In the following dry bulk density is referred to as bulk density (BD). Average bulk density per field was calculated as mean value of the 4 sub-plots.

### **Climate and geology**

Kalomo, Katete and Lusaka are located in the humid subtropical climate, an area with dry winter and hot summer (Beck et al. 2018). During winter, temperatures are high with almost no rainfall between May and August (World Bank 2024b). The wet season between September and April brings intense rainfall controlled by the passage of the tropical rain belt which oscillates between the northern and southern tropics. Annual mean precipitation is lowest in Kalomo (700-750mm), closely followed by Lusaka (750-800mm). Katete receives around 900-1000mm rain per year.

Kalomo's area is generally flat with sandstone as parent material, resulting in sandy Orthic Ferrallosol soils (Glynn et al. 2017). Lusaka's fields, located on the Lusaka plateau, are close to the Ngwerere and Chalimbana streams which brings water and fine material (Japan International Cooperation Agency (JICA) 2009). This has resulted into local textural variations according to the farmers, however, the general soil type was classified as Ferric Luvisols. The sample area in Katete is located around rocky hills of carbonatites and agglomerates rocks (Lee 1974).

Erosion, intense weathering and micro-climates formed diverse soils, generally classified as Ortic Ferraloso.

## 2.2 Determination of hydraulic properties

Two hydraulic properties were measured: field-saturated hydraulic conductivity ( $K_{fs}$ ) and water retention ( $\theta_\psi$ ) as field capacity (at -10kPa) and permanent wilting point (at -1500kPa). To determine  $K_{fs}$ , I adopted the approach used by Bargués-Tobella et al. (2024). In the field, water infiltration rate was measured following the LDSF by applying single-ring infiltration testing under falling-head conditions (see Figure 3). For this, a single-ring infiltrometer consisting of a plastic tube of 120mm diameter and 210mm height with sharpened edges was placed in the centre of each sub-plot, gently pushed into the soil until it entered 20mm in the soil and a ruler was placed vertically in the tube so that it showed the height from the soil surface. Next, water was poured into the tube to pre-wet the soil to get closer to steady-state conditions. After 15 minutes, the tube was re-filled to 18cm above the soil surface and the timer started. In an interval of 5 minutes (and after some time 10 and 20 minutes) the water surface level was recorded and the tube re-filled to 180mm above the soil surface. If the water fully drained before the interval ended, the time was noted and the tube re-filled. In total, a run lasted between 90-180 minutes depending on the rate at which constant infiltration was reached. Infiltration was measured mid-season, hence in February-March.

Infiltration rate measurement points were used to estimate the  $K_{fs}$ , following the methodology demonstrated in Figure 4. To begin, Nimmo et al. (2009)'s formula was applied to account for non-constant falling head and subsurface radial spreading typical of single-ring infiltrometers:

$$K_{fs}^i = \frac{L_G}{\delta t} \ln \left( \frac{L_G + \alpha + D_f}{L_G + \alpha + D_d} \right),$$

where  $K_{fs}^i$  represents an intermediate  $K_{fs}$  still influenced by the suction of soil particles and thus not at full saturation. Furthermore,  $\delta t$  denotes the duration of the time interval (5, 10, or 20 minutes),  $\alpha$  represents the soil macroscopic capillary length (83.33mm (Reynolds & Elrick 1990; Reynolds et al. 2002)),  $D_f$  is the ponding depth of the filled tube (180mm),  $D_d$  is the drained ponding depth after the interval (as recorded) and  $L_G$  the ring-installation scaling length defined by the formula:

$$L_G = C_1 d + C_2 b,$$

where  $C_1$  and  $C_2$  are empirically determined constants (0.316  $\pi$  and 0.184  $\pi$ , respectively (Reynolds et al. 2002)),  $d$  is the ring insertion depth (20mm) and  $b$  the inner tube radius (60mm). The formula by Nimmo et al. (2009) was applied to all recorded infiltration measurements which resulted in a series of decreasing values over time rather than one  $K_{fs}$  per repetition. To determine a final value for  $K_{fs}$ , a



curve was fitted to these points and the asymptotic values were extracted. This task was accomplished using the Python package "lmfit" (Newville et al. 2014) which employs non-linear least squares regression with the Levenberg-Marquardt algorithm, similar to the R code described by Bargués-Tobella et al. (2024). The fitting function was configured to ensure a decreasing trend over time without reaching negative values. An advantage of the "lmfit" model is its ability to automatically terminate the fitting process if the specified criteria mentioned above are not met and its ability to compute metrics such as  $R^2$  and  $\chi^2$  (chi-square).  $R^2$  determines if the data points are randomly distributed or on a trend, typically a value between 0-1 (0: indicating no trend, 1: indicating perfect fit).  $\chi^2$  determines the absolute error compared to the standard deviation (Newville et al. 2014).  $R^2$  and  $\chi^2$  values are computed for each fitted curve per field resulting in 3-4  $R^2$  and  $\chi^2$  values per field. Finally, the mean steady-state  $K_{fs}$  values per field were calculated as median of all sub-plot values. In total, 107  $K_{fs}$  values were generated on 32 fields. It should be noted that on 21 fields only 3 out of 4 sub-plots were sampled for infiltration due to resource constraints.

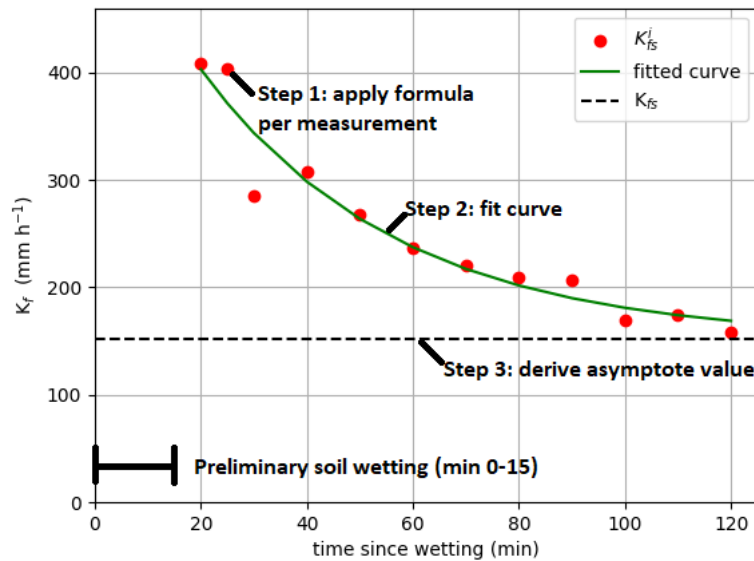


Figure 4: Example of field-saturated hydraulic conductivity ( $K_{fs}$ ) determination.  $K_{fs}^i$  represents an intermediate value where saturation has not fully occurred.  $K_{fs}$  represents the final value used for further assessments.  $K_{fs}$ : field-saturated hydraulic conductivity.

To determine  $\theta_v$ , undisturbed soil samples were gathered in the field using soil cylinders. For this, soil cylinders (72mm diameter) were manufactured by cutting and sharpening plastic tubes. Due to manufacturing inaccuracies, dimensions of cylinders varied between 50-70mm depth. The cylinders were then placed on the soil, covered with a wooden plank, inserted in the soil by gently hammering on the wooden plank with a mallet until the cylinder top reached the soil surface, sealed on the bottom with a trowel by pushing the trowel in the soil from the side, carefully

pulled out, cleaned and sealed with lids. This procedure was repeated 4 times per horizon per field and was always located on the centre sub-plot. The following depths were sampled: 0-5cm and 30-35cm for soils with 2 horizons (horizon A and B) and 0-5cm, 20-25cm, 40-45cm for soils with 3 horizons (horizon A, B<sub>int</sub> and B). Afterwards the samples were taken to the University of Zambia (UNZA) and  $\theta_{\psi}$  was determined using a pressure plate assembly. Water content at the following suction pressures was tested: -10 kPa, correlating with the field capacity (FC) for sandy soils (Richards & Weaver 1944) and -1500 kPa, representing the permanent wilting point (PWP). Further pressure points were not included in this study as they were not predicted by most selected PTFs.

## 2.3 Pedotransfer function selection

Several selection criteria were established for PTF. The primary requirement was that the training data must originate from tropical and humid to arid regions, specifically from Africa, Australia, South America and India. Additionally, the USDA texture classification had to be used for the PTF to be considered and the training dataset for the PTF needed to include at least 100 samples. If the PTF input included organic substances (or fraction thereof), only organic carbon was acceptable, excluding other classes such as organic matter. Finally, in the creation process, PTFs were trained on a specific set of input parameters. I verified that the majority of our results fell within the parameter range.

To identify suitable PTFs, peer-reviewed literature from Clarivate (Web of Science n.d.), Elsevier (Elsevier n.d.), Scopus (Scopus n.d.), Springer publishing (Springer Publishing n.d.) and Wiley (Wiley n.d.) was examined. The search criteria for these databases included keywords, publication time limits (with a preference for functions published after the year 2000) and the criteria mentioned above: geographic region, texture classification, sample-size, class of organic substances and parameter range of training data. The keywords used in the search comprised a combination of terms: pedotransfer function, tropics, Africa, Sub-Saharan, Australia, Brazil, India, Southern Africa, Zambia, saturated hydraulic conductivity and water retention.

In total, 12 PTFs were selected: 3 which return  $K_{fs}$  predictions and 9 which return  $\theta_{\psi}$ , of which, 2 predict the full curve and 7 predict points on the curve at the pressure levels -10kPa and -1500kPa (-33kPa represents FC and -1500kPa the PWP). Table 1 gives an overview on the selected PTFs. It can be seen, that most of the PTFs use texture and organic carbon as main predictor. Bulk density is a less often used predictor (5 out of 12 times) while CEC and pH are only used twice and always in combination with many other variables. Exceptional predictors are N, stoniness and porosity (P). Stoniness in particular was not sampled in this study but, on a

subjective basis from the field excursions, it can be assumed to be low or 0. Similarly, P was not sampled, but it has been calculated using the formula:

$$P = 1 - \left( \frac{\text{bulk density}}{\text{particle density}} \right),$$

where particle density is equal 2.65.

Table 1: Selected pedotransfer functions to be tested with the Zambian agricultural soils.  $\theta_w$ : water retention curve (as soil water content  $\theta_m$  at a certain negative pressure  $m$  (unit: kPa)),  $\theta_{-10, -1500}$  water content at negative pressure levels -10 and -1500,  $K_{fs}$ : field-saturated hydraulic conductivity, cl: clay, si: silt, sa: sand, OC: organic carbon, BD: bulk density, CEC: cation exchange capacity and EP: effective porosity.

Author	Year	Region	Country	Input	Output
Adhikary et al. ( $\theta$ )	2008	tropics	India	cl, si, sa	$\theta_{-10, -1500}$
Adhikary et al. ( $K_{fs}$ )	2008	tropics	India	cl, si	$K_{fs}$
Dijkerman ( $\theta$ )	1988	tropics	Sierra Leone	cl, sa	$\theta_{-1500}$
Gunarathna et al. ( $\theta$ )	2019	tropics	Sri Lanka	si, sa, OC	$\theta_{-10, -1500}$
Hodnett & Tomasella ( $\theta$ )	2002	tropics	world	cl, si, sa, OC, BD, CEC, pH	$\theta_m$
Kalumba et al. ( $K_{fs}$ )	2020	tropics	Zambia	sa, BD, N, stone	$K_{fs}$
Minasny & Hartemink ( $\theta$ )	2011	tropics	world	cl, sa, OC, BD	$\theta_{-10, -1500}$
Myeni et al. ( $\theta$ )	2021	-	South Africa	cl, si, SOC	$\theta_{-1500}$
Otoni et al. ( $K_{fs}$ )	2019	tropics	Brazil & US	cl, si, EP	$K_{fs}$
Santra et al. ( $\theta$ )	2018	arid	India	cl, sa OC	$\theta_{-1500}$
Teferi et al. ( $\theta$ )	2023	tropics	Ethiopia	cl, si, sa, OC, BD, CEC, pH	$\theta_m$
van den Berg et al. ( $\theta$ )	1997	tropics	world Oxisols	cl, si, OC, BD	$\theta_{-10, -1500}$

Table 2 and Figure 5 depict the range of the training data. Sand has the highest range, followed by clay and thereby can fit the data easily. Similarly, most of the bulk density ranges allow for loose soils as well as compacted soils. The range for organic carbon is relatively diverse. Regarding CEC, pH and N, they showed a high range (CEC: 0-94 cmol kg<sup>-1</sup> for Hodnett and Tomase (2002) and 2-85 cmol kg<sup>-1</sup> for Teferi et al. (2023), pH: 3.6-9.6 for Hodnett and Tomase (2002) and 4.2-8.4 for Teferi et al. 2023, N: 0.00-0.37% for Kalumba et al. (2020)).

Table 2: Range of the pedotransfer function training data-set for texture variables. x: no data given in the literature, -: variable not in the function.

Author	clay in %	silt %	sand %	OC %	Dry BD g cm <sup>-3</sup>
Adhikary et al. ( $\theta$ )	3-69	1-52	2-99	-	-
Adhikary et al. ( $K_{fs}$ )	3-69	1-52	-	-	-

Dijkerman ( $\theta$ )	0-70	-	0-100	-	-
Gunarathna et al. ( $\theta$ )	-	0-39	5-99	0.0-4.5	-
Hodnett and Tomase ( $\theta$ )	0-95	0-77	0-99	0.0-30.8	0.3-1.9
Kalumba et al. ( $K_{fs}$ )	-	-	3-97	-	0.8-2.0
Minasny and Hartemink ( $\theta$ )	0-100	-	x	x	0.5-2.0
Myeni et al. ( $\theta$ )	1-83	1-68	-	0.0-11.7	-
Otoni et al. ( $K_{fs}$ )	0-96	0-82	-	0.5-2.0	-
Santra et al. ( $\theta$ )	1-68	-	4-97	0.1-11.0	-
Teferi et al. ( $\theta$ )	4-95	0-70	5-70	0.1-4.9	0.5-1.8
van den Berg et al. ( $\theta$ )	10-95	x	-	0.1-5.2	0.8-1.6

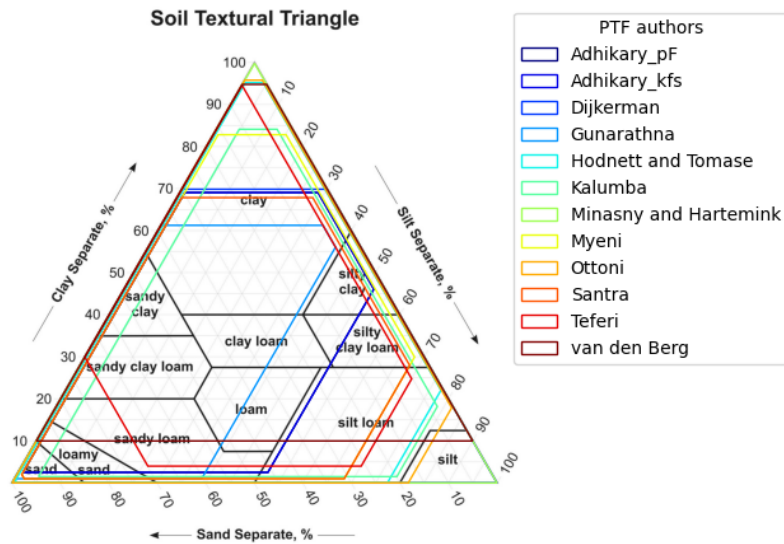


Figure 5: Boundaries of the selected PTF texture input parameters in a texture triangle. If no boundary was given, a boundary of 100% was assumed for the respective value. “Adhikary\_pF”: Adhikary et al. ( $\theta$ ).

## 2.4 Statistical validation

Whether a district had significantly different soil properties compared to another district was determined using a one-way ANOVA analysis. P-values below 0.05 signal significant differences.

To explore the relationships of soil properties with  $K_{fs}$ , a linear regression analysis was conducted. This method connects a single explanatory variable to an independent variable assuming a casual relationship and fits a linear function. The linear relation is expressed numerically with the coefficient of determination ( $R^2$ )

as described above. It is important to note that this method measures only linear correlations and, as such, cannot detect non-linear relationships.

Validation of the PTF performance was performed using 3 statistical parameters: Pearson correlation coefficient (R), mean error (ME) and the root mean square error (RMSE). R determines the relationship between measured and predicted variable, ME gives information on the bias of the relationship and RMSE shows mean absolute deviation. Similar statistics were used in (Stumpp et al. 2009). All statistical parameters in this thesis were computed in Python using the "SciPy" package (Virtanen et al. 2020).

Sensitivity of functions were determined by the simple one-at-a-time (OAT) sensitivity analysis. The OAT analysis plots the change of single input-parameter against the change in output, depicting the sensitivity as rate of change (Pianosi et al. 2016). However, soil parameters are interdependent and changing one parameter affects others. For example, altering the sand content influences the clay and silt content. To account for such cases, 3 scenarios were generated based on the parameters measured in the field: "texture 1", "texture 2" and "OC", all of which are depicted in Figure 6. In the first scenario "texture 1", the silt content is set to 0%, while clay and sand contents are inversely varied between 0-100%. Other required input parameters (e.g. OC) are kept constant at the median of the sampled results from this study. The scenario "texture 2" takes into account variations in silt content between 0-30%. Depending on the silt content, the sand and clay parameter vary between 0-100% and 100-0% respectively, resulting in a quadratic function where:

$$clay = 0.006 * x^2 - 1.6 * x + 100$$

and

$$silt = -0.012 * x^2 + 1.2 * x$$

where:

$$x = \frac{-0.4 + \sqrt{0.4^2 - 4 * 0.006 * (-sand)}}{2 * 0.006}$$

where *sand* is any number between 0-100.

In the last scenario "OC" the texture is fixed at sand=42.5%, silt=15% and clay=42.5%, while the OC content is varied between 0-8%. The sensitivity analysis was plotted in Python using the "seaborn" package (Waskom 2021).

## 2.5 Missing data

Due to issues in the lab and communication difficulties, not all samples were available by the time this thesis was written. The final number of received results is listed in Table 3 and Table 4 under the column "n". The missing data was mostly from Lusaka, where only 5 out of 12 fields were fully evaluated, but also from Katete, where 7 out of 10 fields were fully evaluated except for CEC which was not

measured at all by the lab. Additionally, the physical and chemical samples from Katete were evaluated in a different lab in Malawi. Due to the missing data on the intermediate B horizon ( $B_{int}$ ), it was not included in the following analysis.

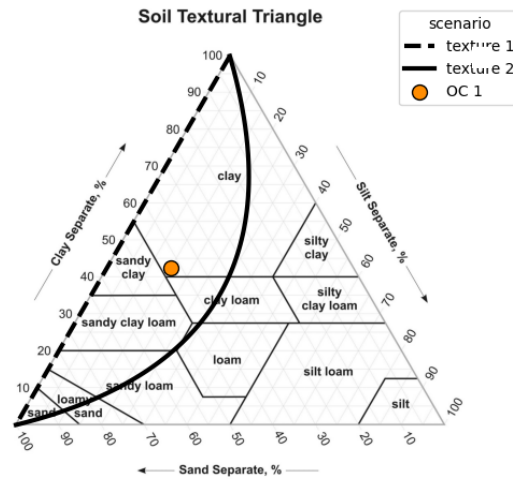


Figure 6: 3 scenarios for the sensitivity analysis, showing the extent of variations on a texture triangle. In scenario “texture 1” and “texture 2” only the texture content is varied while all other variables are kept constant. In scenario “OC” only the organic carbon (OC) content is varied.

## 3. Results

### 3.1 Site description

#### **Farm management**

Typical smallholder farming practices dominated at Kalomo and Katete sites. Through interviews with farmers at time of sampling, I was informed that fields were exclusively rain-fed with no irrigation regime or soil water management installed or planned. Farmers tilled the fields by hand with garden hoes before seeding, affecting the top 20cm soil. Crop-residues from harvest were removed from the fields leaving them bare throughout the dry season while fertilization was only done for maize due to the high cost of fertilizer. Many fields were cultivated for less than 20 years and cleared using the slash-and-burn method. In Kalomo, the predominant crop was maize with little to no crop rotation employed according to farmers. In Katete, crops were rotated more often with maize, soy, sunflower, groundnut and other crops, however maize was still the dominante crop. In Lusaka, soils were managed intensively on large scale farms - so called commercial farms. All sampled fields had overhead sprinkler pivots in combination with soil moisture sensor equipment, modern crop management (including crop-rotation, fertilization, pesticides and herbicides), field soil analyses through commercial laboratories (not available for this study) availability of heavy farm equipment for cultivation, ploughing and other tasks and recovery of crop-residues to the soil.

#### **Soil characteristics and analysis of three sites**

The distribution of soil characteristics per location and depth is depicted in Figure 7. A detailed numerical overview is given in Table 3 and Table 4.

Across all measured fields, clay content varied between 0-94%. Lusaka's site had a significantly higher clay fraction compared to the other fields while also showing high variations between the different fields. This could be related to local texture variations (some owners informed us about natural clay hotspots in their field. There is also effort to adjust field texture by manually introducing sand from other places). With the transition to B horizons, clay content increased in Lusaka and Kalomo while Katete depicted consistently low clay content around 10%.

Silt content remained below 20%, with the exception of some elevated values in horizon A in Lusaka.

The sand fraction dominated the soil composition throughout all horizons at most small-scale farms. Average sand content ranged around 80% in Kalomo and Katete in the horizon A. At deeper layers this value dropped to 60% in Kalomo while remaining at the same level in Katete. In Lusaka average sand content was around 35% and 10% in the horizon A and B, respectively. An outlier in Lusaka showed 100% sand content – an extreme condition that differs greatly from the authors observations in the field and is most likely a measurement error.

OC content varied between 0.11-1.77% across all sampled fields. Average OC content was around 1% for horizon A in Lusaka and Katete and around 0.5% in Kalomo. In horizon B OC generally decreased, however this decrease was more pronounced in Lusaka than in the other locations. Regardless of OC content, a more diverse soil organism population was observed in Lusaka, while soils in Kalomo and Katete showed mostly termite activity at the time of sampling.

Soils in Katete and Kalomo had average BD values of around  $1.4\text{g cm}^{-3}$  in the horizon A which decreased with depth. In Kalomo the decrease was much more moderate but in Katete the variations between the fields ranged from  $1.1\text{-}1.7\text{g cm}^{-3}$  making it difficult to determine a trend. Soils in Lusaka had a different pattern. While the median BD values at the horizon A were between  $1.2\text{-}1.3\text{g cm}^{-3}$ , they increased in depth to around  $1.4\text{g cm}^{-3}$ .

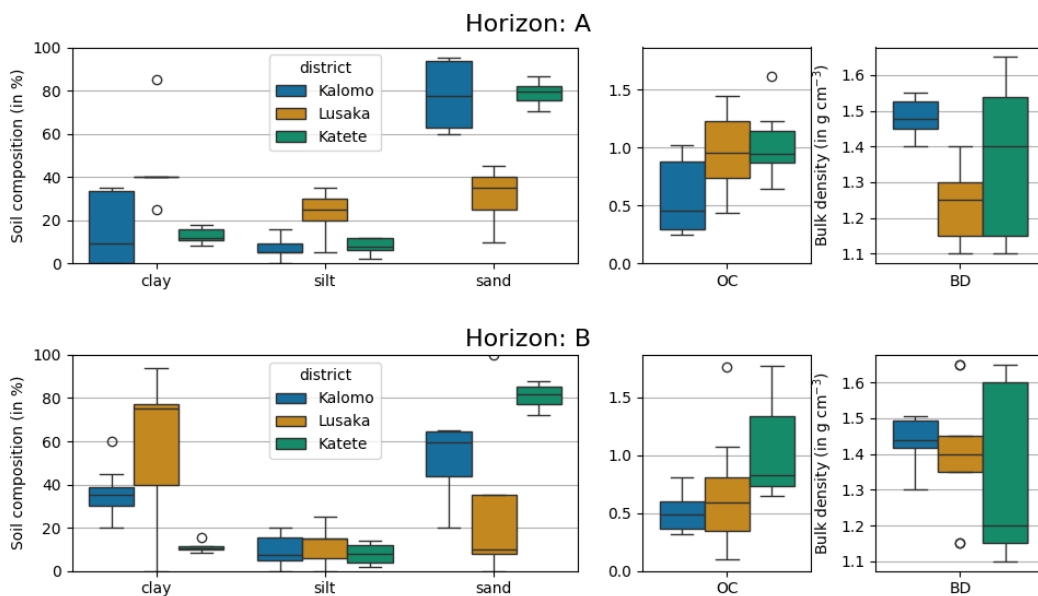


Figure 7: Graphical disaggregation of selected soil properties per district (Kalomo, Lusaka and Katete) and horizon (A and B). OC: organic carbon, BD: bulk density.



Table 3: Chemical and physical data of the sampling sites per A horizon as well as the p-values to determine significant differences between districts (Kalomo, Lusaka and Katete). n: number of samples, OC: organic carbon, BD: bulk density, CEC: cation exchange capacity, N: nitrogen,  $\theta$ : water content at pressure level -10 kPa or -1500 kPa, x: insufficient data of all districts.

Horizon:		A					
Variable	in	min	median	mean	max	p-value	n
clay	%	0	16	26	85	0.003	22
silt	%	0	8	11	35	0.001	22
sand	%	10	75	68	95	2.4E-5	22
OC	%	0.25	0.85	0.84	1.62	0.013	27
BD	g cm <sup>-3</sup>	1.1	1.4	1.4	1.7	0.004	32
CEC	cmol kg <sup>-1</sup>	0.05	0.21	6.47	39.24	X	20
pH	-	4.04	5.94	5.76	6.94	0.762	27
N	%	0.01	0.06	0.06	0.14	8.272	27
$\theta_{-10}$	cm <sup>3</sup> cm <sup>-3</sup>	0.12	0.28	0.27	0.38	0.001	32
$\theta_{-1500}$	cm <sup>3</sup> cm <sup>-3</sup>	0.02	0.08	0.09	0.40	0.024	32

Table 4: Chemical and physical data of the sampling sites per B horizon as well as the p-values to determine significant differences between districts (Kalomo, Lusaka and Katete). n: number of samples, OC: organic carbon, BD: bulk density, CEC: cation exchange capacity, N: nitrogen,  $\theta$ : water content at pressure level -10 kPa or -1500 kPa, x: insufficient data of all districts.

Horizon:		B					
Variable	in	min	median	mean	max	p-value	n
clay	%	0	31	33	94	0.002	22
silt	%	0	9	10	25	0.607	22
sand	%	0	64	57	100	0.003	22
OC	%	0.11	0.62	0.71	1.77	0.032	27
BD	g cm <sup>-3</sup>	1.1	1.4	1.4	1.7	0.509	32
CEC	cmol kg <sup>-1</sup>	0.03	0.10	5.43	30.77	X	20
pH	-	4.10	6.01	5.66	6.79	7.0E-8	27
N	%	0.01	0.04	0.05	0.15	0.002	27
$\theta_{-10}$	cm <sup>3</sup> cm <sup>-3</sup>	0.13	0.29	0.30	0.52	2.0E-4	32
$\theta_{-1500}$	cm <sup>3</sup> cm <sup>-3</sup>	0.05	0.09	0.13	0.24	1.0E-4	32

### Soil water retention

The most water was retained in Lusaka with an average water content of 0.3 cm<sup>3</sup> cm<sup>-3</sup> at FC and 0.1 cm<sup>3</sup> cm<sup>-3</sup> at PWP in horizon A, increasing to 0.4 cm<sup>3</sup> cm<sup>-3</sup> and 0.2 cm<sup>3</sup> cm<sup>-3</sup> in horizon B at FC and PWP, respectively (see Figure 8). Similar trends were observed across the other districts, with a significant difference between districts. Nevertheless, the relative difference between districts declined. At horizon A, the water content at the PWP was almost identical between Lusaka

and Katete although texture was remarkably different (with clay content of 40% and 13% respectively).

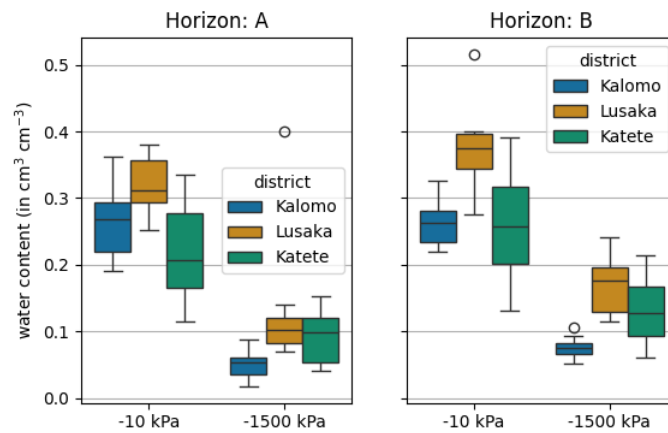


Figure 8: Graphical disaggregation of hydraulic properties per district (Kalomo, Lusaka and Katete) and horizon (A and B). -10 kPa: field capacity, -1500 kPa: permanent wilting point.

### Field infiltration measurement and field-saturated hydraulic conductivity

Unsaturated infiltration rates were lowest in Katete and Kalomo. Top-Figure 9 depicts this observation, whereas each colour represents one field with 3-4 repetitions (by running several measurements at the same time) and the solid lines represent the average. At both sites, the infiltration rate remained relatively constant and did not decrease strongly since the first measurement point. This might be related to some rainfall occurring shortly before the sampling in Katete, while no rain was recorded prior to the other districts. The exception were 2 sites in Katete which displayed fast infiltration over time, however there is no visible difference in texture, OC or BD. This decline might be explained by the presence of earth channels (e.g., from termites), which could have enhanced water flow. In Lusaka the infiltration rate was even stronger with large decreases over time and major differences between each repetition.

Regarding the curve fitting procedure of  $K_{fs}^i$  points,  $R^2$  values were low at some Kalomo sites, indicating that no trend of measurement over time emerged but rather that measurement points were randomly distributed (see centre Figure 9). In Katete,  $R^2$  values scored better while the best  $R^2$  values can be found in Lusaka. Chi-square values were lowest in Kalomo, followed by Katete, indicating that the points were close to the curve. Lusaka's soils showed higher fluctuation in the measurement points, which can be partly attributed to the generally higher values.

Finally, median  $K_{fs}$  per field ranged from 3 to 210  $\text{mm h}^{-1}$  (see bottom Figure 9). Katete's soils showed the lowest median  $K_{fs}$  with 7 soils being below 50  $\text{mm h}^{-1}$ , except for 2 sites which had median  $K_{fs}$  of 121 and 189  $\text{mm h}^{-1}$ . In Kalomo, measured values were moderately rapid to rapid from 33 to 141  $\text{mm h}^{-1}$ . In Lusaka

the soils had the highest median  $K_{fs}$  but also the highest variation within a field. In 5 instances the variation within a field reached over  $150 \text{ mm h}^{-1}$  with the maximum variation being  $243 \text{ mm h}^{-1}$ . The overall median per district differed significantly between districts ( $p\text{-value} = 0.002$ ), with lowest values in Katete ( $46 \text{ mm h}^{-1}$ ), likely due to wet sampling conditions, followed by Kalomo ( $72 \text{ mm h}^{-1}$ ) and Lusaka ( $134 \text{ mm h}^{-1}$ ).

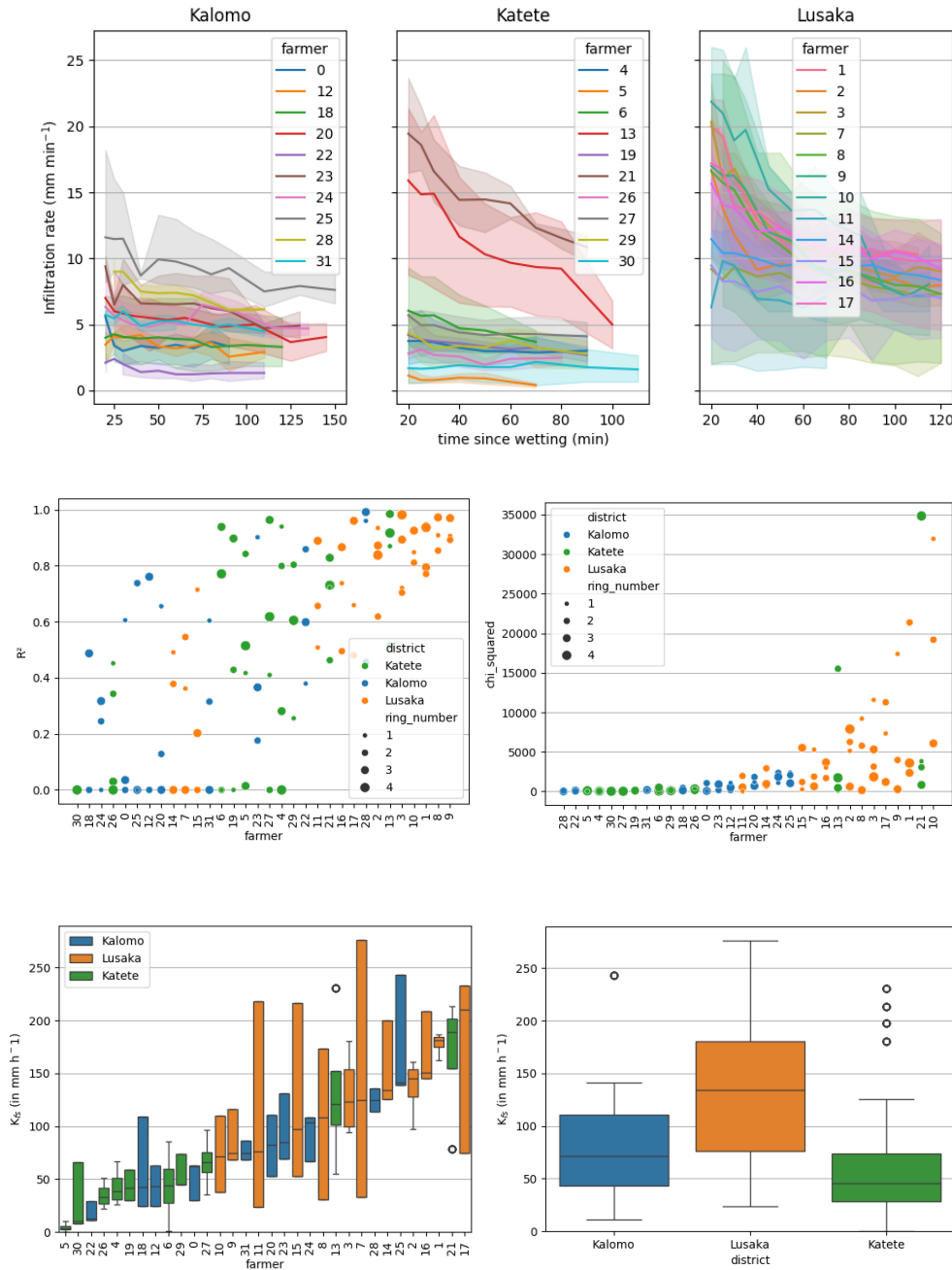


Figure 9: Field-saturated hydraulic conductivity ( $K_{fs}$ ) results per location (Katete, Kalomo and Lusaka). Top: Mean infiltration rates with 95% confidence interval of the 3-4 repeated infiltration measurements per sampled field. Centre: statistical results from the curve fitting procedure to estimate the randomness of measured points. Bottom: final  $K_{fs}$  distribution per field and per district.

### 3.2 Predictors for field-saturated hydraulic conductivity

Simple linear regression analysis results for horizon A are depicted in Figure 10. In the instances of silt and sand content, the resulting linear function was close to diagonal, indicating a correlation between these parameters and  $K_{fs}$ . This was confirmed by the  $R^2$ , which was 0.40 and 0.28 for the silt and the sand correlation respectively. Other variables, such as clay content, OC content and BD, both the regression analysis and the  $R^2$  showed poor predicting capabilities.

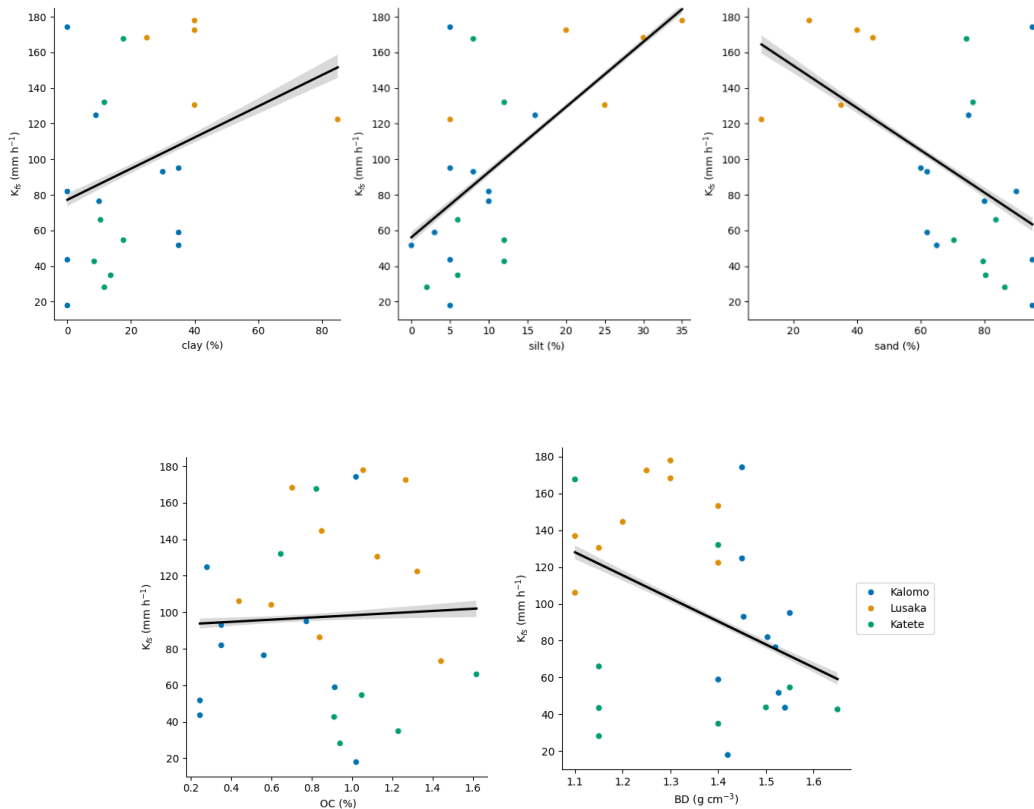


Figure 10: Simple linear regression plots of selected variables and field-saturated hydraulic conductivity ( $K_{fs}$ ) at horizon A. The regression line shown in the plots was calculated across all districts but only for horizon A. OC: organic carbon, BD: bulk density.

### 3.3 Accuracy of selected pedotransfer functions

The statistical comparison of the  $K_{fs}$  prediction via PTFs and the observation are presented in Table 5 and graphically depicted in Figure 11. All 3  $K_{fs}$ -predicting PTFs had R values below 0 demonstrating little predicting capabilities. Adhikary et al. (2008) and Ottoni et al. (2019) returned values below roughly 50 mm h<sup>-1</sup> although more than half of the observed values exceeded this threshold. Such low values can be attributed to their PTFs, which were calibrated primarily with Kfs

values below  $50 \text{ mm h}^{-1}$  and only predict higher values at very high sand concentrations (roughly at 90% and more). Kalumba et al. (2020) predicted values of high  $K_{fs}$  however, with no overall correlation. The PTF's high dependency on stone and sand content made it prone to high infiltration rates, whereas the only reducing factors in the function are bulk density and N. The weak correlation is also visible when plotting the observed data against the predicted data: the scatter plot reveals a random distribution of points, with no discernible pattern or trend. The lack of alignment along any line indicates that the predictions do not correspond well with the actual observations. Consequently, ME and RMSE values were high for all cases.

Table 5: Evaluation of the predicted field-saturated hydraulic conductivity ( $K_{fs}$ ) for top-soil (horizon A).

Author	R	RMSE	ME
Adhikary ( $K_{fs}$ )	-0.23	101.49	61.14
Kalumba ( $K_{fs}$ )	-0.15	105.17	-74.57
Otoni ( $K_{fs}$ )	-0.28	84.11	61.13

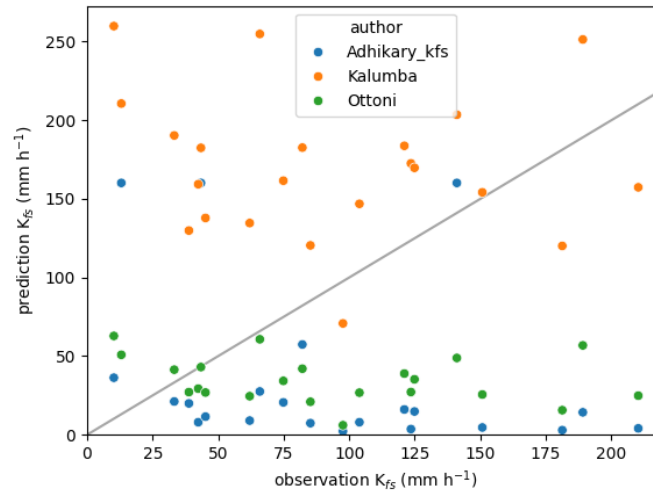


Figure 11: Performance of pedotransfer functions which return field-saturated hydraulic conductivity ( $K_{fs}$ ) for top-soil (horizon A) conditions. The grey line represents the 1:1 agreement where points would lie if the predictions exactly matched the observations.

PTFs on water content were also tested on their predictability. The results are shown in Table 6 and Figure 12. Generally, all PTFs except the one from Teferi et al. (2023) showed a positive R value, ranging from 0.19 to 0.49, suggesting that the PTFs were able to reproduce the observations to some extent. The best R value was achieved by Gunarathna et al. (2019), followed by van den Berg (1997) and Hodnett and Tomase (2002). Most PTFs performed better at horizon A than horizon B, while the difference between FC (-10 kPa) and PWP (-1500 kPa) varied between the

functions. At FC, most of the predicted values ranged from 0.1 to 0.4  $\text{cm}^3 \text{cm}^{-3}$ , the same range as the observation. At PWP, a noticeable outlier-cluster between 0.15 and 0.35  $\text{cm}^3 \text{cm}^{-3}$  formed, although most observations didn't exceed 0.15  $\text{cm}^3 \text{cm}^{-3}$ . This cluster represented farms with elevated clay content. A closer analysis of the PTFs revealed a clear trend: as expected, soils with a greater proportion of fine particles tend to retain more water at PWP.

Table 6: Evaluation of the predicted water retention at field capacity (-10 kPa) and permanent wilting point (-1500 kPa) per horizon A and B.

Author	pressure (in -kPa)	A			B		
		R	RMSE	ME	R	RMSE	ME
Adhikary ( $\theta$ )	10	0.41	0.12	0.04	0.40	0.13	0.01
Adhikary ( $\theta$ )	1500	0.27	0.10	-0.02	0.29	0.10	-0.03
Dijkerman ( $\theta$ )	1500	0.31	0.08	-0.03	0.26	0.10	-0.06
Gunarathna ( $\theta$ )	10	0.37	0.09	0.02	0.37	0.09	0.02
Gunarathna ( $\theta$ )	1500	0.49	0.09	-0.06	0.36	0.09	-0.06
Hodnett and Tomase( $\theta$ )	10	0.41	0.13	0.10	0.24	0.11	0.08
Hodnett and Tomase( $\theta$ )	1500	0.40	0.11	-0.05	0.42	0.11	-0.08
Minasny and Hartemink( $\theta$ )	10	0.38	0.08	-0.02	0.35	0.09	-0.02
Minasny and Hartemink( $\theta$ )	1500	0.34	0.11	-0.06	0.19	0.12	-0.08
Myeni ( $\theta$ )	1500	0.40	0.07	-0.02	0.31	0.08	-0.04
Santra ( $\theta$ )	1500	0.33	0.06	-0.01	0.31	0.08	-0.03
Teferi ( $\theta$ )	10	-0.22	0.15	-0.10	-0.71	0.14	-0.01
Teferi ( $\theta$ )	1500	-0.45	0.24	-0.17	-0.69	0.17	-0.11
van den Berg ( $\theta$ )	10	0.41	0.08	0.03	0.43	0.09	0.03
van den Berg ( $\theta$ )	1500	0.44	0.08	-0.03	0.32	0.08	-0.03

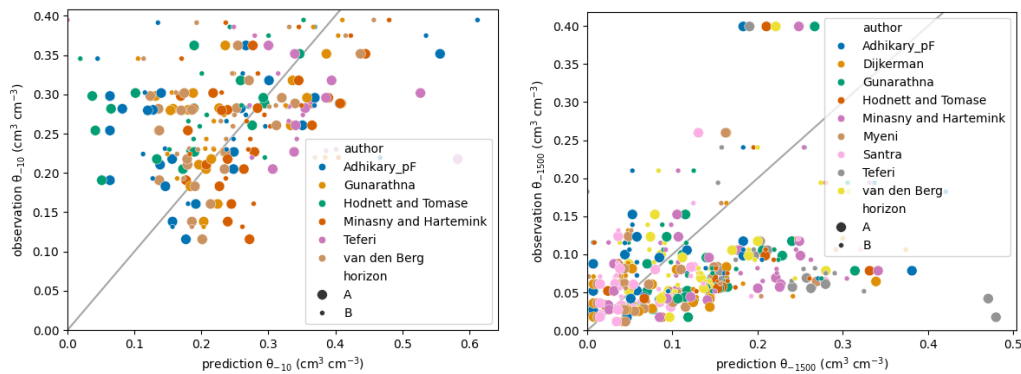


Figure 12: Performance of pedotransfer functions which return the water content ( $\theta$ ) for top-soil (horizon A) conditions. The grey line represents the 1:1 line agreement where points would lie if the predictions exactly matched the observations.

### 3.4 Sensitivity of selected pedotransfer functions

Sensitivity of PTFs was determined based on the 3 scenarios "texture 1", "texture 2" and "OC", calculated as change compared to 50% sand or OC content and depicted in Figure 13 and Figure 14. Adhikary et al. (2008)'s function for predicting  $K_{fs}$  was increasingly sensitive with higher sand content especially at sand content exceeding 80%. This is related to low  $K_{fs}$  values at 50% sand content. Since silt and OC were no input variables, the scenario "texture 2" was identical to "texture 1" and the scenario "OC" was not relevant. Kalumba et al. (2020) showed a simple linear increase with  $\pm 60\%$  change compared to the 50% sand content. Ottoni et al. (2019) had a similar behaviour with little difference between the texture scenarios, indicating that silt and clay behave similar according to the function. All  $K_{fs}$ -predicting PTFs predicted increasing  $K_{fs}$  with higher sand content.

The majority of water retention predicting PTFs demonstrated a high sensitivity towards sand content. The higher the sand content, the lower the water retention capacity. Inversely, the higher the clay content, the higher the water retention. For scenario "texture 1", in 8 out of 9 PTFs the change in output was linear or close to linear with the change in sand content. In 3 PTFs, the output decreased significantly at sand content close to 100% reaching below a tenth of retention at 50% sand content. In 3 other PTFs the change was only moderate. The difference in output between FC (-10 kPa) and PWP (-1500 kPa) was little for 7 PTFs with a difference of around 10%, showing low sensitivity on the applied suction pressure. If silt content was present (as in scenario "texture 2"), water retention decreased compared to no silt. The silt replaced the clay fraction, which itself had a significantly higher water retention capacity. In 6 out of 9 PTFs the change in output was strong when silt content reached its maximum. More than half the change in output was visible when silt reached 30% compared to no silt. In 4 PTFs, water retention decreased stronger with higher negative pressures compared to no silt, indicating that silt has a higher impact at higher negative pressures. For the last scenario "OC", which varies the OC content between 0-8%, the change in output was modest. In 6 out of 7 PTFs (only 7 PTFs used OC as input parameter) output changed between  $\pm 25\%$  at 0 or 8% OC content compared to 4% OC content. Differences between negative pressures were only visible for 3 PTFs, where higher OC content improved water retention at stronger negative pressures. It should be mentioned however, that this scenario assumes that the other parameters are constant. The sensitivity of OC might change when assuming other constant input parameters.

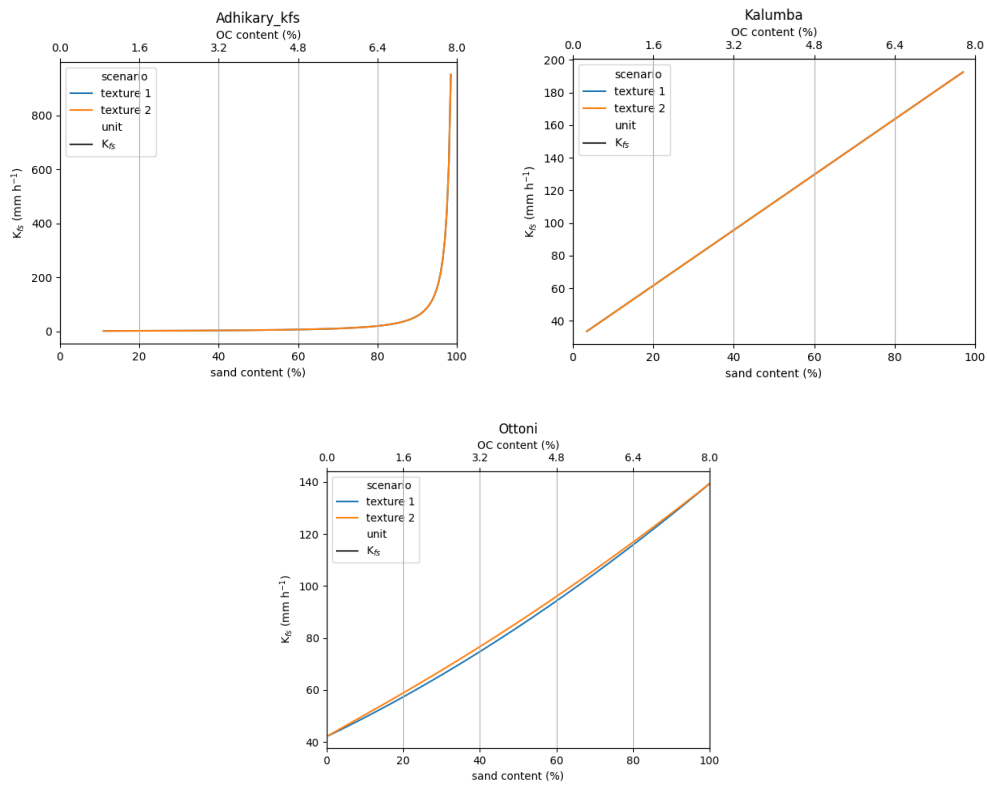
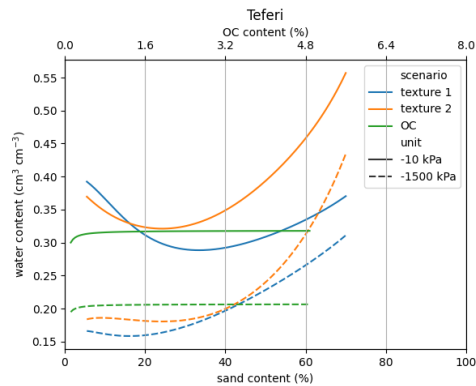
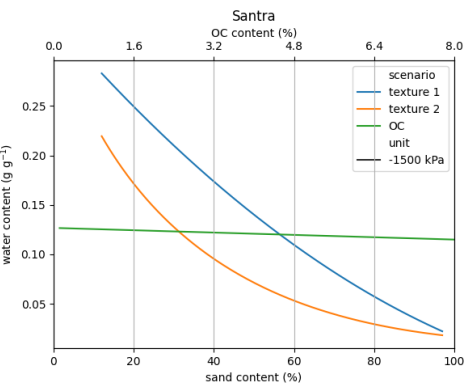
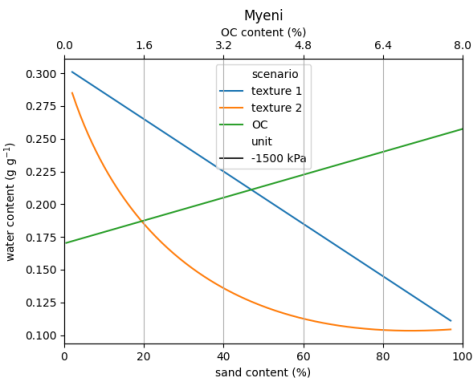
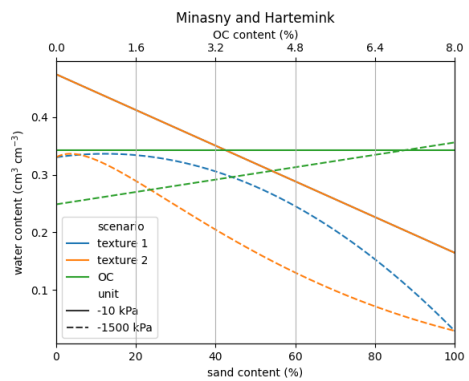
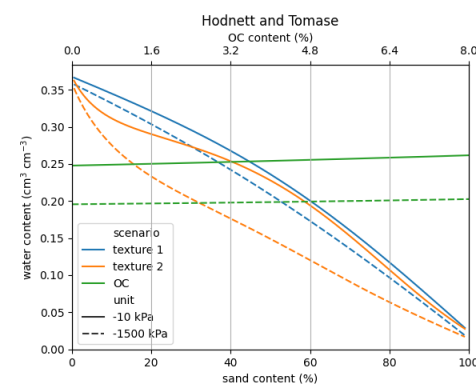
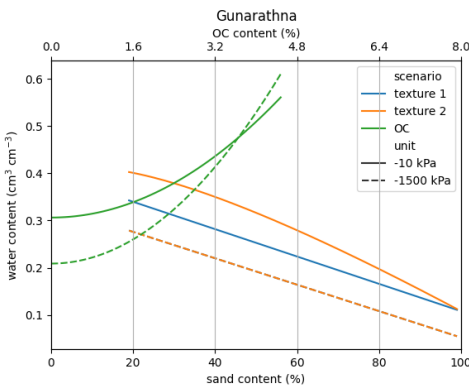
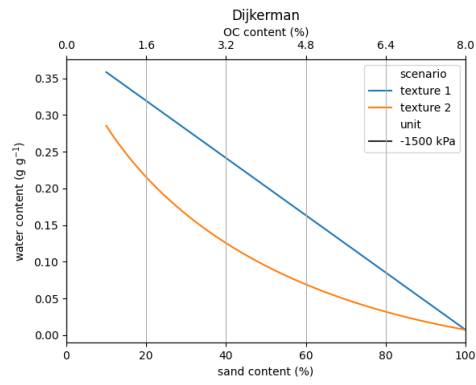
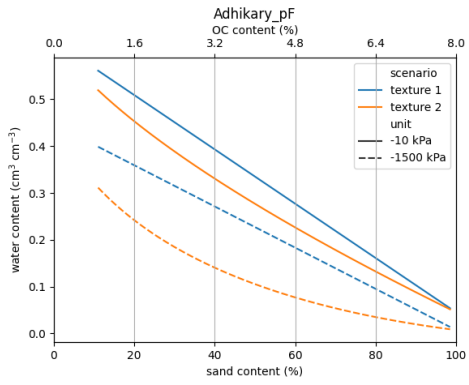


Figure 13: Sensitivity analysis of pedotransfer functions which return field-saturated hydraulic conductivity values. The y-axis represents the variation in field-saturated hydraulic conductivity.





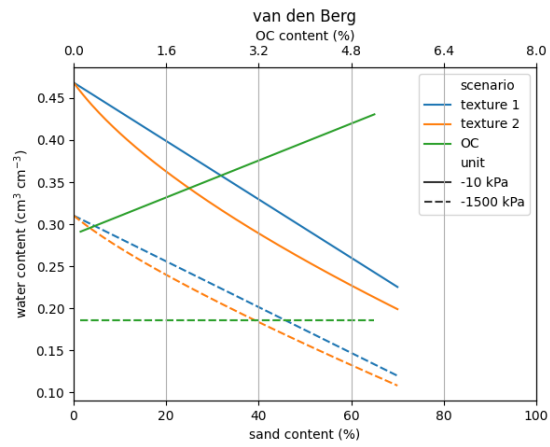


Figure 14: Sensitivity analysis of pedotransfer functions which return water retention values. The y-axis represents the variation in water content given by the functions. OC: organic carbon.

## 4. Discussion

### **Limitations in methods and material**

The methods employed in this study (including the LDSF) were effective in capturing soil characteristics, nevertheless certain limitations became apparent during the sampling process and subsequent data analysis.

The prolonged dry weather conditions complicated sampling with the cylinders and the auger. In sandy soils, the lack of moisture caused particles to become loose, making cohesive sample collection difficult. In contrast, clay and silty soils clumped and broke apart when stressed. Future studies should pre-wet soils, even just slightly, to stabilize structure and improve measurement reliability.

The sampling sessions were conducted several months and years apart. Over this period, chemical properties were prone to variations and follow-up sampling was complicated due to difficulties in locating previous sites. This turned out to be important in fields with high spatial variabilities of texture like Lusaka and Katete, increasing uncertainties in the correlation between measured variables. Timely sampling for consistent samples and recording of geo-coordinates is recommended.

An advantage of conducting field work is, to compare lab data with the impressions in the field to identify outliers and explain certain behaviours. In this study, a larger number of discrepancies between in-field observations and lab data were observed: soils in Kalomo appeared significantly more sandy than in Katete during the fieldwork, while it was the other way around according to the lab results. Lusaka's soils appeared to have high OC content in horizon A and elevated fine particle content in sub horizons. Bulk density appeared homogeneous in Katete. These discrepancies likely reduced correlations between variables and decreased performance of predictive functions. However, even with these issues, the data gives a first impression on the soils behaviour in the area.

### **Results and comparison to literature**

Estimated  $K_{fs}$  in Kalomo, Katete and Lusaka are consistent with the values presented in other studies (Gupta et al. 2021; Bargués-Tobella et al. 2024; Falk et al. 2024). Bargués-Tobella et al. (2024) recorded median  $K_{fs}$  values between 6-161 mm h<sup>-1</sup> with higher  $K_{fs}$  values exhibiting higher variability in general. However, identified  $K_{fs}$  predictors differed between this study and certain literature. Gupta et

al. (2021) and Bargués-Tobella et al. (2024) found a positive relationship between  $K_{fs}$ , sand content and OC content, while my findings suggested the opposite: higher sand and silt content reduced infiltration while OC and BD had little impact. Other literature suggested that clay particles tend to form cracks when drying, improving infiltration initially, until the cracks are closed, which however takes some time (Dudal 1989; Mavimbela & van Rensburg 2017). For this study  $K_{fs}$  is likely more related to different weather conditions during sampling resulting in the presence of cracks, to soil management and to crust formation, rather than texture.

The second research question focused on evaluating existing PTFs. The selected PTFs demonstrated little ability in predicting observed  $K_{fs}$  and modest prediction capacities for water retention. A possible explanation is that the selected PTFs were not developed for agricultural soils. Bálková et al. (2023), demonstrated that some commonly used and well developed PTFs were unable to give a satisfactory prediction of  $K_{fs}$  on agricultural soils compared to PTFs specifically developed for agriculture. The changes in the pore system due to tillage operations and, thus, the great temporal variability, made it difficult to determine predictors. Differing results could also be related to field-saturation. The selected PTFs determined saturated hydraulic conductivity in the lab which can yield significantly different results (Gupta et al. 2021). It should be mentioned, that water retention estimation in clay rich soils (mainly Lusaka) at PWP underperformed. At 40% clay a water content of  $0.2 \text{ cm}^3 \text{ cm}^{-3}$  and above is expected at PWP (Rab et al. 2009; O'Geen 2013). This increased the difficulties in accurately measuring the PTF prediction capacities. The question arises whether PTFs from different continents can be used for the given setting. However, several studies have done well in predicting water retention in Sub-Sahara African countries with foreign PTFs (Botula et al. 2012; Myeni et al. 2021; Miti et al. 2023).

### **Implications for farming and future science**

This research has shown the complexities in determining hydraulic predictors on agricultural soils. Basic soil properties, such as texture, were insufficient for accurate prediction, implying the existence of other major driving factors. Introducing perennials, tillage and crop management are among the factors which impact infiltration rates the most (Basche & DeLonge 2019; Basset et al. 2023). These factor should not be neglected by farmers and should be taken into account in future studies, while also taking note of spatial and annual variabilities.

Existing PTFs performed questionably, nevertheless they remain a cost effective tool. PTF improvements could be obtained from the inclusion of parameters such as land-use, farming type and crop development stage. Nevertheless, more development of PTFs for agricultural soils in Sub-Saharan Africa is necessary. Transdisciplinary work between farmers and scientists will help to advance soil research and management practices.

## References

- Adepoju, P. (2021). Africa worst hit by climate change impacts, COP26 told. *Nature Africa*,. <https://doi.org/10.1038/d44148-021-00107-z>
- Adhikary, P.P., Chakraborty, D., Kalra, N., Sachdev, C.B., Patra, A.K., Kumar, S., Tomar, R.K., Chandna, P., Raghav, D., Agrawal, K. & Sehgal, M. (2008). Pedotransfer functions for predicting the hydraulic properties of Indian soils. *Soil Research*, 46 (5), 476–484. <https://doi.org/10.1071/SR07042>
- Aina, P.O. & Periaswamy, S.P. (1985). Estimating available water-holding capacity of western Nigerian soils from soil texture and bulk density, using core and sieved samples. *Soil Science*, 140 (1), 55
- Bargués-Tobella, A., Winowiecki, L.A., Sheil, D. & Vågen, T.-G. (2024). Determinants of Soil Field-Saturated Hydraulic Conductivity Across Sub-Saharan Africa: Texture and Beyond. *Water Resources Research*, 60 (1), e2023WR035510. <https://doi.org/10.1029/2023WR035510>
- Basche, A.D. & DeLonge, M.S. (2019). Comparing infiltration rates in soils managed with conventional and alternative farming methods: A meta-analysis. *PLOS ONE*, 14 (9), e0215702. <https://doi.org/10.1371/journal.pone.0215702>
- Basset, C., Abou Najm, M., Ghezzehei, T., Hao, X. & Daccache, A. (2023). How does soil structure affect water infiltration? A meta-data systematic review. *Soil and Tillage Research*, 226, 105577. <https://doi.org/10.1016/j.still.2022.105577>
- Báťková, K., Matula, S., Miháliková, M., Hružová, E., Abebrese, D.K., Serdar Kara, R. & Almaz, C. (2023). Prediction of saturated hydraulic conductivity Ks of agricultural soil using pedotransfer functions. *Soil and Water Research*, 18 (1), 25–32. <https://doi.org/10.17221/130/2022-SWR>
- Beck, H.E., Zimmermann, N.E., McVicar, T.R., Vergopolan, N., Berg, A. & Wood, E.F. (2018). Present and future Köppen-Geiger climate classification maps at 1-km resolution. *Scientific Data*, 5 (1), 180214. <https://doi.org/10.1038/sdata.2018.214>
- van den Berg, M., Klamt, E., van Reeuwijk, L.P. & Sombroek, W.G. (1997). Pedotransfer functions for the estimation of moisture retention characteristics of Ferralsols and related soils. *Geoderma*, 78 (3), 161–180. [https://doi.org/10.1016/S0016-7061\(97\)00045-1](https://doi.org/10.1016/S0016-7061(97)00045-1)
- Botula, Y.-D., Cornelis, W.M., Baert, G. & Van Ranst, E. (2012). Evaluation of pedotransfer functions for predicting water retention of soils in Lower Congo (D.R. Congo). *Agricultural Water Management*, 111, 1–10. <https://doi.org/10.1016/j.agwat.2012.04.006>
- Chikowo, R. (2024). *Zambia - Global yield gap atlas*. <https://www.yieldgap.org/zambia> [2024-08-05]
- Dijkerman, J.C. (1988). An Ustult-Aquult-Tropept catena in Sierra Leone, West Africa, II. Land qualities and land evaluation. *Geoderma*, 42 (1), 29–49. [https://doi.org/10.1016/0016-7061\(88\)90021-3](https://doi.org/10.1016/0016-7061(88)90021-3)
- Dudal, R. (1989). Vertisols of subhumid and humid zones., 1989. 55–59 Elsevier (n.d.). *Elsevier | An Information Analytics Business*. [www.elsevier.com](http://www.elsevier.com). <https://www.elsevier.com> [2024-07-16]

- EM-DAT & CRED (2024). EM-DAT Drought Disaster Occurrences: Africa query. UCLouvain, Brussels, Belgium. <https://public.emdat.be/>
- Falk, D., Winowiecki, L.A., Vågen, T.-G., Lohbeck, M., Ilstedt, U., Muriuki, J., Mwaniki, A. & Bargués Tobella, A. (2024). Drivers of field-saturated soil hydraulic conductivity: Implications for restoring degraded tropical landscapes. *Science of The Total Environment*, 907, 168038. <https://doi.org/10.1016/j.scitotenv.2023.168038>
- GLOSOLAN (2019). Standard operating procedure for soil organic carbon. Walkley-Black method: titration and colorimetric method. Food and Agriculture Organization of the United Nations. <https://openknowledge.fao.org/server/api/core/bitstreams/e498d73e-1711-4d18-9183-aa8476387e2c/content>
- Glynn, S.M., Master, S., Wiedenbeck, M., Davis, D.W., Kramers, J.D., Belyanin, G.A., Frei, D. & Oberthür, T. (2017). The Proterozoic Choma-Kalomo Block, SE Zambia: Exotic terrane or a reworked segment of the Zimbabwe Craton? *Precambrian Research*, 298, 421–438. <https://doi.org/10.1016/j.precamres.2017.06.020>
- Gunarathna, M.H.J.P., Sakai, K., Nakandakari, T., Momii, K., Kumari, M.K.N. & Amarasekara, M.G.T.S. (2019). Pedotransfer functions to estimate hydraulic properties of tropical Sri Lankan soils. *Soil and Tillage Research*, 190, 109–119. <https://doi.org/10.1016/j.still.2019.02.009>
- Gupta, S., Hengl, T., Lehmann, P., Bonetti, S. & Or, D. (2021). SoilKsatDB: global database of soil saturated hydraulic conductivity measurements for geoscience applications. *Earth System Science Data*, 13 (4), 1593–1612. <https://doi.org/10.5194/essd-13-1593-2021>
- Hartemink, A.E. (2002). Soil Science in Tropical and Temperate Regions—Some Differences and Similarities. In: Sparks, D.L. (ed.) *Advances in Agronomy*. Academic Press. 269–292. [https://doi.org/10.1016/S0065-2113\(02\)77016-8](https://doi.org/10.1016/S0065-2113(02)77016-8)
- Hodnett, M.G. & Tomasella, J. (2002). Marked differences between van Genuchten soil water-retention parameters for temperate and tropical soils: a new water-retention pedo-transfer functions developed for tropical soils. *Geoderma*, 108 (3), 155–180. [https://doi.org/10.1016/S0016-7061\(02\)00105-2](https://doi.org/10.1016/S0016-7061(02)00105-2)
- IPCC (2022). *Climate Change 2022: Impacts, Adaptation and Vulnerability*. Cambridge University Press.
- Jägermeyr, J., Gerten, D., Schaphoff, S., Heinke, J., Lucht, W. & Rockström, J. (2016). Integrated crop water management might sustainably halve the global food gap. *Environmental Research Letters*, 11 (2), 025002. <https://doi.org/10.1088/1748-9326/11/2/025002>
- Japan International Cooperation Agency (JICA) (2009). *The Study on Comprehensive Urban Development Plan for the City of Lusaka in the Republic of Zambia: Final Report*. JICA. [https://openjicareport.jica.go.jp/pdf/11928512\\_01.pdf](https://openjicareport.jica.go.jp/pdf/11928512_01.pdf)
- Kalumba, M., Bamps, B., Nyambe, I., Dondeyne, S. & Van Orshoven, J. (2021). Development and functional evaluation of pedotransfer functions for soil hydraulic properties for the Zambezi River Basin. *European Journal of Soil Science*, 72 (4), 1559–1574. <https://doi.org/10.1111/ejss.13077>
- Karlsson, I. (1982). Soil moisture investigation and classification of seven soils in the Mbeya Region, Tanzania., 1982. <https://www.semanticscholar.org/paper/Soil-moisture-investigation-and-classification-of-Karlsson/f4b0d1f1844e892a173ab992112a4252c518fc20> [2024-08-08]

- Kjeldahl, J. (1883). Neue Methode zur Bestimmung des Stickstoffs in organischen Körpern. *Zeitschrift für analytische Chemie*, 22 (1), 366–382. <https://doi.org/10.1007/BF01338151>
- Lal, R. (1978). Physical properties and moisture retention characteristics of some nigerian soils. *Geoderma*, 21 (3), 209–223. [https://doi.org/10.1016/0016-7061\(78\)90028-9](https://doi.org/10.1016/0016-7061(78)90028-9)
- Lee, C.A. (1974). The geology of the Katete carbonatite, Rhodesia. *Geological Magazine*, 111 (2), 133–142. <https://doi.org/10.1017/S0016756800038176>
- Lehmann, J., Bossio, D.A., Kögel-Knabner, I. & Rillig, M.C. (2020). The concept and future prospects of soil health. *Nature Reviews Earth & Environment*, 1 (10), 544–553. <https://doi.org/10.1038/s43017-020-0080-8>
- Mavimbela, S.S.W. & van Rensburg, L.D. (2017). Characterizing infiltration and internal drainage of South African dryland soils. *Earth Surface Processes and Landforms*, 42 (3), 414–425. <https://doi.org/10.1002/esp.3991>
- Minasny, B. & Hartemink, A.E. (2011). Predicting soil properties in the tropics. *Earth-Science Reviews*, 106 (1), 52–62. <https://doi.org/10.1016/j.earscirev.2011.01.005>
- Minasny, B. & McBratney, A.B. (2018). Limited effect of organic matter on soil available water capacity. *European Journal of Soil Science*, 69 (1), 39–47. <https://doi.org/10.1111/ejss.12475>
- Miti, C., Mbanyele, V., Mtangadura, T., Magwero, N., Namaona, W., Njira, K., Sandram, I., Lubinga, P.N., Chisanga, C.B., Nalivata, P.C., Chimungu, J.G., Nezomba, H., Phiri, E. & Lark, R.M. (2023). The appraisal of pedotransfer functions with legacy data; an example from southern Africa. *Geoderma*, 439, 116661. <https://doi.org/10.1016/j.geoderma.2023.116661>
- Mukumbuta, I., Chabala, L.M., Sichinga, S., Miti, C. & Lark, R.M. (2021). A comparison between three legacy soil maps of Zambia at national scale: The spatial patterns of legend units and their relation to soil properties. *Geoderma*, 402, 115193. <https://doi.org/10.1016/j.geoderma.2021.115193>
- Myeni, L., Mdlambuzi, T., Paterson, D.G., De Nysschen, G. & Moeletsi, M.E. (2021). Development and Evaluation of Pedotransfer Functions to Estimate Soil Moisture Content at Field Capacity and Permanent Wilting Point for South African Soils. *Water*, 13 (19), 2639. <https://doi.org/10.3390/w13192639>
- Newville, M., Stensitzki, T., Allen, D.B. & Ingargiola, A. (2014). *LMFIT: Non-Linear Least-Square Minimization and Curve-Fitting for Python* (0.8.0). Zenodo. <https://doi.org/10.5281/zenodo.11813>
- Ngoma, H., Hamududu, B., Hangoma, P., Samboko, P. & Kabaghe, C. (2019). IRRIGATION DEVELOPMENT FOR CLIMATE RESILIENCE IN ZAMBIA: THE KNOWN KNOWN AND KNOWN UNKNOWN. *AgEcon search*, 144, 49. <https://doi.org/10.22004/ag.econ.303048>
- Nimmo, J.R., Schmidt, K.M., Perkins, K.S. & Stock, J.D. (2009). Rapid Measurement of Field-Saturated Hydraulic Conductivity for Areal Characterization. *Vadose Zone Journal*, 8 (1), 142–149. <https://doi.org/10.2136/vzj2007.0159>
- Nkiaka, E., Bryant, R.G., Okumah, M. & Gomo, F.F. (2021). Water security in sub-Saharan Africa: Understanding the status of sustainable development goal 6. *WIREs Water*, 8 (6), e1552. <https://doi.org/10.1002/wat2.1552>
- O’Geen, A.T. (2013). Soil Water Dynamics. *Nature Education Knowledge*, 4 (5), 9
- Otoni, M.V., Otoni Filho, T.B., Lopes-Assad, M.L.R.C. & Rotunno Filho, O.C. (2019). Pedotransfer functions for saturated hydraulic conductivity using a database with temperate and tropical climate soils. *Journal of Hydrology*, 575, 1345–1358. <https://doi.org/10.1016/j.jhydrol.2019.05.050>

- Pianosi, F., Beven, K., Freer, J., Hall, J.W., Rougier, J., Stephenson, D.B. & Wagener, T. (2016). Sensitivity analysis of environmental models: A systematic review with practical workflow. *Environmental Modelling & Software*, 79, 214–232. <https://doi.org/10.1016/j.envsoft.2016.02.008>
- Pidgeon, J.D. (1972). The Measurement and Prediction of Available Water Capacity of Ferrallitic Soils in Uganda. *Journal of Soil Science*, 23 (4), 431–441. <https://doi.org/10.1111/j.1365-2389.1972.tb01674.x>
- Rab, M.A., Fisher, P.D., Armstrong, R.D., Abuzar, M., Robinson, N.J. & Chandra, S. (2009). Advances in precision agriculture in south-eastern Australia. IV. Spatial variability in plant-available water capacity of soil and its relationship with yield in site-specific management zones. *Crop and Pasture Science*, 60 (9), 885–900. <https://doi.org/10.1071/CP08350>
- Reynolds, D., Elrick, D. & Youngs, E. (2002). Ring or cylinder infiltrometers (vadose zone). *Methods of soil analysis*, 818–826
- Reynolds, W.D. & Elrick, D.E. (1990). Poned Infiltration From a Single Ring: I. Analysis of Steady Flow. *Soil Science Society of America Journal*, 54 (5), 1233–1241. <https://doi.org/10.2136/sssaj1990.03615995005400050006x>
- Richards, L.A. & Weaver, L. (1944). Moisture retention by some irrigated soils as related to soil-moisture tension., February 18 1944. <https://www.semanticscholar.org/paper/Moisture-retention-by-some-irrigated-soils-as-to-Richards-Weaver/ddafcf35a7cec7976066e288aa5e0efe080b57d6> [2024-08-05]
- Rockström, J., Karlberg, L., Wani, S.P., Barron, J., Hatibu, N., Oweis, T., Bruggeman, A., Farahani, J. & Qiang, Z. (2010). Managing water in rainfed agriculture—The need for a paradigm shift. *Agricultural Water Management*, 97 (4), 543–550. <https://doi.org/10.1016/j.agwat.2009.09.009>
- Santra, P., Kumar, M., Kumawat, R.N., Painuli, D.K., Hati, K.M., Heuvelink, G.B.M. & Batjes, N.H. (2018). Pedotransfer functions to estimate soil water content at field capacity and permanent wilting point in hot Arid Western India. *Journal of Earth System Science*, 127 (3), 35. <https://doi.org/10.1007/s12040-018-0937-0>
- Schollenberger, C.J. & Simon, R.H. (1945). DETERMINATION OF EXCHANGE CAPACITY AND EXCHANGEABLE BASES IN SOIL—AMMONIUM ACETATE METHOD: *Soil Science*, 59 (1), 13–24. <https://doi.org/10.1097/00010694-194501000-00004>
- Scopus (n.d.). *Scopus - Document search*. <https://www.scopus.com/search/form.uri?display=basic#basic> [2024-07-16]
- Silva, J.V., Baudron, F., Ngoma, H., Nyagumbo, I., Simutowe, E., Kalala, K., Habeenzu, M., Mphatso, M. & Thierfelder, C. (2023). Narrowing maize yield gaps across smallholder farming systems in Zambia: what interventions, where, and for whom? *Agronomy for Sustainable Development*, 43 (2), 26. <https://doi.org/10.1007/s13593-023-00872-1>
- Springer Publishing (n.d.). *Springer Link*. <https://link.springer.com/>
- Stumpp, C., Engelhardt, S., Hofmann, M. & Huwe, B. (2009). Evaluation of pedotransfer functions for estimating soil hydraulic properties of prevalent soils in a catchment of the Bavarian Alps. *European Journal of Forest Research*, 128 (6), 609–620. <https://doi.org/10.1007/s10342-008-0241-7>
- Tamene, L., Sileshi, G.W., Ndengu, G., Mponela, P., Kihara, J., Sila, A. & Tondoh, J. (2019). Soil structural degradation and nutrient limitations across land use categories and climatic zones in Southern Africa. *Land Degradation & Development*, 30 (11), 1288–1299. <https://doi.org/10.1002/ldr.3302>
- Teferi, E., O'Donnell, G., Kassawmar, T., Mersha, B.D. & Ayele, G.T. (2023). Enhanced Soil Moisture Retrieval through Integrating Satellite Data with



- Pedotransfer Functions in a Complex Landscape of Ethiopia. *Water*, 15 (19), 3396. <https://doi.org/10.3390/w15193396>
- Teschemacher, C., Ng'ombe, T., Fajardo-Steinhäuser, M. & Wani, S. (2024). What constrains agricultural productivity in Zambia? International Growth Centre (IGC). <https://www.theigc.org/sites/default/files/2024-02/13286%20Policy%20Framing%20Paper%20What%20constrains%20agricultural%20productivity%20in%20Zambia%20%28final%29.pdf>
- Vågen, T.-G. & Winowiecki, L.A. (2023). The LDSF Field Manual - Land and Soil Health Assessments using the Land Degradation Surveillance Framework (LDSF). Center for International Forestry Research (CIFOR).
- Van Looy, K., Bouma, J., Herbst, M., Koestel, J., Minasny, B., Mishra, U., Montzka, C., Nemes, A., Pachepsky, Y.A., Padarian, J., Schaap, M.G., Tóth, B., Verhoef, A., Vanderborght, J., van der Ploeg, M.J., Weihermüller, L., Zacharias, S., Zhang, Y. & Vereecken, H. (2017). Pedotransfer Functions in Earth System Science: Challenges and Perspectives. *Reviews of Geophysics*, 55 (4), 1199–1256. <https://doi.org/10.1002/2017RG000581>
- Vereecken, H., Weynants, M., Javaux, M., Pachepsky, Y., Schaap, M.G. & van Genuchten, M.Th. (2010). Using Pedotransfer Functions to Estimate the van Genuchten–Mualem Soil Hydraulic Properties: A Review. *Vadose Zone Journal*, 9 (4), 795–820. <https://doi.org/10.2136/vzj2010.0045>
- Virtanen, P., Gommers, R., Oliphant, T.E., Haberland, M., Reddy, T., Cournapeau, D., Burovski, E., Peterson, P., Weckesser, W., Bright, J., van der Walt, S.J., Brett, M., Wilson, J., Millman, K.J., Mayorov, N., Nelson, A.R.J., Jones, E., Kern, R., Larson, E., Carey, C.J., Polat, İ., Feng, Y., Moore, E.W., VanderPlas, J., Laxalde, D., Perktold, J., Cimrman, R., Henriksen, I., Quintero, E.A., Harris, C.R., Archibald, A.M., Ribeiro, A.H., Pedregosa, F., van Mulbregt, P., & SciPy 1.0 Contributors (2020). SciPy 1.0: Fundamental Algorithms for Scientific Computing in Python. *Nature Methods*, 17, 261–272. <https://doi.org/10.1038/s41592-019-0686-2>
- Waskom, M.L. (2021). seaborn: statistical data visualization. *Journal of Open Source Software*, 6 (60), 3021. <https://doi.org/10.21105/joss.03021>
- Web of Science (n.d.). *Web of Science Core Collection*. <https://www.webofscience.com/wos/woscc/basic-search> [2024-07-16]
- Wiley (n.d.). *Wiley Online Library*. *Wiley Online Library*. <https://onlinelibrary.wiley.com/> [2024-07-16]
- World Bank (2024a). Labor force, total - Zambia. World Development Indicators database. <https://data.worldbank.org/indicator/SL.TLF.TOTL.IN?locations=ZM> [2024-08-05]
- World Bank (2024b). *World Bank Climate Change Knowledge Portal*. <https://climateknowledgeportal.worldbank.org/> [2024-10-20]
- Young, M.D.B., Gowing, J.W., Hatibu, N., Mahoo, H.M.F. & Payton, R.W. (1999). Assessment and development of pedotransfer functions for semi-arid sub-Saharan Africa. *Physics and Chemistry of the Earth, Part B: Hydrology, Oceans and Atmosphere*, 24 (7), 845–849. [https://doi.org/10.1016/S1464-1909\(99\)00091-X](https://doi.org/10.1016/S1464-1909(99)00091-X)
- Zambia Statistics Agency (2023). 2022 Annual Labour Force Survey Report. Republic of Zambia, Ministry of Labour and Social Security.

## Popular science summary

In future, farmers in Africa will have less usable water due to climate change. Most farmers do not have the tools and money to handle the big weather changes and instead depend on soil to soak up rain and keep the water for the crops to grow. Scientists have developed Pedotransfer functions (PTFs) to estimate how much water soils can retain, but they do not work for all soils. Only few of such PTFs have actually been tested for African soils. In this work, I tested twelve PTFs on their accuracy for agricultural soils in Zambia, Africa. Therefore, 32 fields in 3 districts and 2 farming systems (“traditional” small-scale farms and commercial farms) were sampled for soil texture, organic matter, bulk density, water retention and for field-saturated hydraulic conductivity ( $K_{fs}$ ) in top and subsoil.

I found, that water infiltrated the soil faster on commercial farms compared to small-scale farms (about twice the rate), while the soil on commercial farms also had finer texture (mean clay content= 40%). A reason might be that there were cracks in the soil due to the texture and management practices and that the water flowed into the cracks, infiltrating the soil quicker.

When looking for PTFs to estimate soil water flow ( $K_{fs}$ ), I found few that worked well. The PTFs, I tried gave very different results from what was measured in the field, they did not predict  $K_{fs}$  accurately.

For estimating soil water retention, I found more PTFs that seemed suitable, but their accuracy was inconsistent. For field capacity, the accuracy range was  $-0.21 < R < 0.41$  for topsoil and  $-0.71 < R < 0.40$  for subsoil. For the wilting point, it was  $-0.45 < R < 0.49$  (topsoil) and  $-0.69 < R < 0.42$  (subsoil). Errors were particularly high for wilting points above 0.15 vol%, possibly due to lab errors at high pressures.

These results show a need to look beyond basic soil tests for better water flow estimates. More field data is needed to improve PTF accuracy for Zambian farms.

## Acknowledgements

This study was supported by the LEG4DEV research project [<https://leg4dev.org/>] (European Commission's Directorate-General for International Partnerships (DG INTPA) Development Smart Innovation through Research in Agriculture (DeSIRA) Initiative (Grant Ref: FOOD/2020/418-901)). This study was supported by the International Institute of Tropical Agriculture, which provided support with transportation. The field work was only possible due to all participating farmers in Kalomo, Katete and Lusaka, who allowed this work to be conducted on their fields.

Big thanks goes to the lead researcher Emmanuel Ngonga who planned and realized the field sampling and who enriched my experiences in Africa. Thank you also to my supervisors Jennie Barron and Christine Stumpp who always gave constructive feedback on the progress. Thank you Mario Feifel for the opposition after its presentation and the feedback on the work.

I want to thank my family: Martina who is the cause of my motivation to go to Africa, my parents who supported me from home, and my relatives whom were interested. Most of all I want to thank my partner, who reviewed my work, who gave me hope and who has the biggest heart on earth!

## Publishing and archiving

Approved students' theses at SLU are published electronically. As a student, you have the copyright to your own work and need to approve the electronic publishing. If you check the box for **YES**, the full text (pdf file) and metadata will be visible and searchable online. If you check the box for **NO**, only the metadata and the abstract will be visible and searchable online. Nevertheless, when the document is uploaded it will still be archived as a digital file. If you are more than one author, the checked box will be applied to all authors. You will find a link to SLU's publishing agreement here:

- <https://libanswers.slu.se/en/faq/228318>.

YES, I/we hereby give permission to publish the present thesis in accordance with the SLU agreement regarding the transfer of the right to publish a work.

NO, I/we do not give permission to publish the present work. The work will still be archived and its metadata and abstract will be visible and searchable.